HHS Public Access

Author manuscript

Health Phys. Author manuscript; available in PMC 2020 March 01.

Published in final edited form as:

Health Phys. 2019 March ; 116(3): 426–446. doi:10.1097/HP.0000000000000932.

Histopathological features of the development of intestine and mesenteric lymph node injury in a nonhuman primate model of partial-body irradiation with minimal bone marrow sparing

George A. Parker[a], **Na Li**[a], **Kyle Takayama**[a], **Cath Booth**[b], **Gregory L. Tudor**[b], **Ann M. Farese**[c], and **Thomas J. MacVittie**[c]

[a]Charles River Laboratories/Pathology Associates, Durham, NC, USA

[b]Epistem Ltd, Manchester, UK

[c]University of Maryland, School of Medicine, Dept. of Radiation Oncology, Baltimore, MD, USA

Abstract

Male rhesus macaques were subjected to partial-body irradiation at 10, 11, or 12 Gy with 5% bone marrow protection. Animals were euthanized when dictated by prospectively determined clinical parameters, or at approximately 180 days following irradiation. Histological sections of jejunum, colon and mesenteric lymph node were stained with hematoxylin and eosin as well as a battery of histochemical and immunohistochemical stains. The immediate post-irradiation histopathological alterations in the jejunum and colon were based primarily on injury to rapidly proliferating crypt epithelial cells, though there was evidence of additional radiation-induced fibrogenic responses. There was substantial resolution of the radiation-related mucosal injury through the observation period, but microscopically visible defects in mucosal structure persisted to the end of the observation period. In the later stages of the observation period the jejunum and colon had overt fibrosis that was most commonly located in the submucosa and serosa, with less microscopically discernible involvement of the mucosa. Mesenteric lymph nodes had an immediate post-irradiation reduction in cellularity due to the known effects of irradiation on lymphoid cell populations. In later stages of the observation period the lymph nodes also developed fibrotic changes, possibly related to transmigration of immunomodulatory cells and/or signaling molecules from the radiation-damaged intestine.

INTRODUCTION

Delayed effects of acute radiation exposure (DEARE) are a known complication of radiation therapy, and are anticipated to be a contributor to overall morbidity and mortality associated with accidental or deliberate exposure to ionizing radiation. The goal of the current study was to determine the histopathological progress of radiation-associated alterations in the jejunum, colon and mesenteric lymph nodes of male rhesus macaques for approximately 180 days following radiation exposure.

Corresponding author: George A. Parker, Charles River Laboratories-Pathology Associates, 4025 Stirrup Creek Drive, Suite 150, Durham, NC 27703 Telephone: 919-206-7036, FAX: 919-206-7001, george.parker@crl.com.

METHODS

Male rhesus macaques, ranging in age from 3.5 to 9.8 years, mean age = 5.4 years, were exposed to 6 MV Linear Accelerator (LINAC) photon radiation, at a dose rate of 0.80 Gy min^{-1} for a total dose of 10, 11 or 12 Gy, with 5% bone marrow sparing. Animals received supportive clinical care, including dexamethasone and antibiotic administration, in compliance with prospectively delineated clinical parameters. All studies were conducted under an IACUC-approved protocol. Animals were euthanized when necessitated by IACUC-approved clinical condition and humane considerations. Tissue specimens from six non-irradiated animals with no sham treatment, of the same approximate age (mean age = 4.5 years) as the irradiated animals, were used for comparison to the tissue specimens from the irradiated animals.

Specimens of jejunum, colon and mesenteric lymph node were fixed in neutral-buffered formalin at the time of necropsy. Tissues were processed to paraffin blocks via routine histology procedures, and hematoxylin and eosin (H&E)-stained sections were examined by light microscopy. Histological sections subjected to additional histochemical and immunohistochemical staining procedures were prepared and examined (Table 1). Treatment groups were known to the pathologist at the time of histopathological examination.

Methods for histochemical staining were derived from published methods: toluidine blue (Carson 1997), Masson's trichrome (Bancroft and Stevens 1996), periodic acid-Schiff/alcian blue (Sheehan and Hrapchak 1980), and Lendrum's stain (Lendrum 1947).

Immunohistochemical staining was performed on 5μm thick formalin-fixed paraffin embedded sections using the Discovery XT and Discovery Ultra research instruments (Ventana Medical Systems). Sections were deparaffinized with Discovery EZ prep (Ventana Medical Systems), and then either heat retrieved with proprietary solutions Discovery RiboCC and Discovery CC1, or pretreated with Protease 2 (Ventana Medical Systems) at 37˚C. Whenever blocking was needed, Blocking Sniper (Biocare Medical) was applied for between 4 to 8 minutes as pre-determined empirically during assay optimization. Sections were incubated with primary antibodies diluted in Antibody Diluent (Life Technologies) at varying concentrations, temperature and time based on protocols optimized with positive control tissues. Primary antibodies included anti-alpha smooth muscle actin (αSMA) (abcam, AB119952), anti-tryptase (abcam, AB81703), anti-MxA (abcam, AB95926), anti-lipopolysaccharide (LPS)-core (Hycult Biotech, HM6011), anti-Ki-67 (abcam, AB15580), anti-myeloperoxidase (MPO) (abcam, AB9535), anti-CD3 (abcam, AB16669), anti-CD13 (abcam, AB108310), anti-Bmi-1 (Novus Biologicals, NB100–87026), anti-IL22 (abcam, AB 18499), anti-IL22RA1 (Sigma Aldrich, HPA042399), anti-collagen I (abcam, AB34710), anti-transforming growth factor-beta (TGFβ) (abcam, AB92486), and anti-connective tissue growth factor (CTGF) (abcam, AB6992). Sections were then labelled with horseradish peroxidase (HRP)-conjugated secondary antibodies [OmniMap anti-rabbit HRP or OmniMap anti-mouse HRP (Ventana Medical Systems)], and then detected with the ChromoMap diaminobenzidine (DAB) kit (Ventana Medical Systems) prior to counterstaining with hematoxylin and bluing reagent (Ventana Medical Systems).

The stained histological sections were examined by light microscopy and observations were entered in Provantis histopathology data system. Histopathology data entries for selected histological changes were transferred into Microsoft Excel® worksheets for further analysis and generation of illustrative graphs.

Histopathological alterations were recorded using currently accepted diagnostic terminology to the extent possible. In order to convey the extent of histological alterations, each observation was given a subjectively determined severity grade of 1 to 5, with Grade 1 being the least pronounced alteration. A severity grade of zero indicates the histological alteration was not discernible in the sections. Tissue alterations in the irradiated animals were compared to equivalent sections taken from naïve control animals. The severity grades should be interpreted as subjective division of continuous data into ordinal classes, for the purpose of comparing the apparent degree of changes, rather than an attempt at morphometric analysis of the histological changes.

RESULTS

There was a clear radiation dose-associated reduction in survival time which was most pronounced in animals irradiated at the 12 Gy level Table 2). Debilitation in animals euthanized within the first 30 days post-irradiation was largely related to gastrointestinal injury, as indicated by hydration status and overall clinical status (MacVittie et al. 2012, MacVittie et al. 2012). Debilitation in animals in the later stages of the study were largely related to pulmonary injury, as indicated by increased respiratory rate and decreased pO_2 levels.

The development of histological changes was based on necropsy dates, which were determined by clinical presentation of the animals rather than a predetermined termination schedule. For that reason, the results presented herein should not be interpreted as a true time course study of lesion development, but rather an approximation of the lesion development schedule as afforded by specimen availability. The incidences of histological alterations presented below are based on availability of suitably preserved and stained sections rather than the number of animals in each radiation dose cohort, thus there are numerical variations based on technical issues with tissue fixation and staining procedures.

A histological section showing the histomorphological features of the small intestine of a naïve control male rhesus macaque is included for orientation of those who do not routinely deal with histology nomenclature (Figure 1a).

Jejunum- (Figures 1b, 1c, 1d, 1e, 2a, 2b, 2c, 2d, 2e, and 3a, 3b, 3c)

The study was based on animals that reached a predetermined clinical status at the time of sacrifice, as opposed to prospectively determined sacrifice intervals, but it was nevertheless possible to construct a sequence of radiation-related histological alterations in the intestinal mucosa. The most pronounced histological change in the jejunum was epithelial depletion that ranged in severity from Grade 2 to 4, with most changes assigned grades 3 or 4. The most pronounced histological alterations were in animals irradiated at 12 Gy, but similar but less pronounced epithelial depletion was noted in animals irradiated at 10 or 11 Gy. These

changes were considered to be a major contributor to the shorter survival time of animals in this group. Epithelial depletion was noted most commonly during the 40 days following irradiation, but there was evidence of epithelial depletion persisting through the end of the study. The jejunum of a few animals had areas in which the surface epithelium was completely lost, which was recorded as denudation. Blunting and/or fusion of villi consisted of an architectural malformation wherein villi were short and thick, rather than having the long, finger-like contour that is normally seen, or were fused to the surface of adjacent villi.

Inflammatory cell infiltration was notably sparse relative to the degree of epithelial disruption. This was presumed to be a result of radiation effects on the hematopoietic system.

Masson's trichrome staining (Figure 3d) was used for the detection of the fibrosis, which was subcategorized based on the location in the mucosa, submucosa, serosa or muscularis externa. An early stage of fibrosis in the submucosa of the jejunum was present as early as post-irradiation day 8 in an animal irradiated at 12 Gy. Serosal fibrosis typically occurred in animals that had submucosal fibrosis, but not all animals with submucosal fibrosis had concurrent serosal fibrosis. It was interesting to note the external muscular layers (muscularis externa) most commonly had no histological evidence of fibrosis, suggesting the serosal reaction was not an extension of the submucosal reaction. The submucosal and serosal fibrosis tended to be focally or multifocally distributed in the histological sections, suggesting there were local variations in radiation exposure level or tissue reaction to irradiation.

Proliferating crypt cell populations were detected by immunohistochemical staining for Ki67, a marker for cells actively involved in DNA synthesis (Figure 4a, 4b, 4c, 4d, 4e). There was a dramatic reduction in proliferative crypt cells immediately following irradiation, particularly in animals irradiated at 12 Gy, to the extent that jejunal specimens from animals necropsied at post-irradiation day 6 had virtually no evidence of crypt cell proliferation (Figure 4b). Niches of proliferative cells were clearly visible within crypts by post-irradiation day 9, and by day 10 the proliferating cells were spreading across the denuded luminal surface of the jejunum (Figure 4c). At post-irradiation day 29 the population of proliferating crypt epithelial cells was equal to, and perhaps slightly increased over, the proliferative cell population in naïve control animals (Figure 4d). The proliferative cells extended a proportionately greater distance up the sides of villi than was observed in naïve control animals, suggesting the rate of migration of newly formed epithelial cells was increased over that seen in naïve control animals. The proliferative cell population had returned to a normal status at post-irradiation day 77 (Figure 4e).

LPS core immunohistochemical stain- (Figure 5a)

Staining for lipopolysaccharide (LPS) core antigen was subcategorized according to the location in the lamina propria or submucosa of the jejunum. The naïve control animals had no evidence of LPS core^{+} cells in either the lamina propria or the submucosa. The irradiated animals commonly had LPS core^{+} cells in the lamina propria but, despite the obvious radiation-associated damage to the mucosa, only three animals had LPS core^{+} cells in the submucosa. This observation correlates with the absence of demonstrable LPS in blood

samples in the present study (data not shown). LPS core$^+$ bacteria were sometimes present on the mucosal surface, thus serving as an internal control for the immunohistochemical staining procedure.

MxA immunohistochemical stain- (Figure 5b)

Immunohistochemical staining for MxA in leukocyte populations was subcategorized as mucosal or submucosal, based on the location in the histological sections. Mucosal staining for MxA$^+$ cells, assigned grades 1 and 2, was noted in all of the naïve control animals. More pronounced mucosal MxA staining (grades 3 or 4), was noted in the mucosal lamina propria of a number of irradiated animals. The increased level of MxA$^+$ cells was an indication of activated immunocyte populations involved in inflammatory processes secondary to the radiation injury.

Paneth cell populations- (Figures 5c, d)

Paneth cell populations in intestinal crypts were identified by the Lendrum histochemical stain, which imparts a brilliant magenta color to the cytoplasmic granules of Paneth cells. The Paneth cell population was of particular interest due to its known role in maintenance of the intestinal microbiome (Salzman 2010). In the present study, Paneth cell populations in jejunal crypts were markedly reduced following irradiation, particularly at the 12 Gy level, and gradually returned to histologically normal status as the intestinal mucosa was regenerated.

CD13 immunohistochemical stain- (Figures 6a, 6b, 6c)

CD13 is expressed by most cells of myeloid origin, including monocytes, macrophages and granulocytes, and is prominently expressed by the brush border of intestinal epithelial cells. Positive staining for CD13 was consistently observed in the superficial brush border of intestinal epithelial cells of naïve control animals, and there was a pronounced reduction in CD13$^+$ brush border staining in animals that had radiation-associated epithelial depletion or denudation of the jejunum. The CD13$^+$ brush border of intestinal epithelial was regained as the mucosal surface became repopulated by mature epithelial cells. A grade 1–2 population of CD13$^+$ large mononuclear cells, consistent with macrophages, was present in the mucosal lamina propria of three animals irradiated at 12 Gy and necropsied on days 9–17. A similar grade 2 population of CD13$^+$ cells was present in the jejunal mucosa of one animal irradiated at 10 Gy and necropsied on day 182. However, the sparse involvement of CD13$^+$ leukocytes suggested that myeloid-origin cells were not prominently involved in the post-irradiation intestinal alterations.

Collagen 1 immunohistochemical stain- (Figures 6d, e)

Increased collagen staining was subcategorized based on location in the mucosa, submucosa, muscularis externa, or serosa of the jejunal specimens. The level of collagen staining observed in jejunal specimens from the naive controls was used as a baseline (grade of 0) for the subjective determination of increased collagen staining in specimens from the irradiated animals. Increased mucosal collagen staining was noted in a subpopulation of animals from all irradiated groups, but was most frequently noted in animals irradiated at 12 Gy. The

increased mucosal collagen staining was most commonly assigned grade 2, with occasional specimens assigned grades 1, 3, or 4. It should be noted that increased collagen staining in the various sub-locations of the jejunum, but particularly the serosa, tended to be multifocally distributed. Only two specimens from the mid-jejunum were examined microscopically, thus it is likely examination of additional jejunal specimens would reveal additional examples of increased collagen staining.

Connective tissue growth factor (CTGF) immunohistochemical stain- (Figures 7a, b)

Immunohistochemical staining for connective tissue growth factor (CTGF) was noted primarily in the jejunal crypt epithelial cells, with occasional staining in leukocyte/ macrophage populations of the lamina propria. CTGF staining in jejunal crypt epithelial cells of the naive control animals was assigned grade 2 in five of six animals and grade 3 in the remaining animal. A reduced level of CTGF staining in jejunal crypts was commonly associated with depletion and/or denudation of the mucosal epithelium, particularly in animals that were necropsied within 30 days of radiation exposure. As with TGFβ staining (below), animals that were necropsied during the early post-irradiation period but had little microscopic evidence of mucosal epithelial depletion or denudation tended to have substantial levels of CTGF staining in crypt epithelial cells. CTGF staining was largely localized to the deep aspects of crypts, where Paneth cells are located, but it was not clear whether Paneth cells were the sole source of CTGF expression.

Mast cell populations

Mast cell populations were identified by both toluidine blue staining and tryptase immunohistochemical staining. Mast cells were present at grade 1 level in the jejunum of all naïve control animals with toluidine blue staining and 5 of 6 animals with tryptase staining. The remaining tryptase-stained animal had a grade 2 mast cell population in the jejunum. There was no definitive radiation-related variation in the pattern of mast cell populations, but it was noted that mast cell populations in irradiated animals necropsied in the first 30 days post-irradiation commonly had no mast cells visible by toluidine blue staining. This effect was not apparent upon tryptase immunohistochemical staining. Tryptase immunohistochemical staining revealed a slightly greater population of mast cells in the jejunum than was revealed by toluidine blue staining. This was expected, as the toluidine blue staining is known to reveal only the connective tissue mast cell population, and does not include the mucosal mast cell population unless special fixatives are used at the time of tissue collection (Strobel et al. 1981, Enerback 1987). It should be noted that toluidine blue selectively stains the contents of mast cell granules, revealing metachromasia that is based on the carbohydrate contents of the granules, therefore, degranulated mast cells may not be revealed by toluidine blue staining. The tryptase immunohistochemical stain also targets tryptase contained in mast cell granules but, given the exquisite sensitivity of immunohistochemical staining, it is less likely that tryptase immunohistochemical staining would give false negative indications due to mast cell degranulation.

Alpha smooth muscle actin immunohistochemical stain

Immunohistochemical staining for alpha smooth muscle actin (α-SMA) was subcategorized as mucosal, submucosal or serosal. Increased α-SMA staining was rarely noted.

Myeloperoxidase (MPO) immunohistochemical stain (Figure 7c)

Immunohistochemical staining for MPO in jejunal specimens was subcategorized as mucosal or submucosal, primarily indicating MPO^+ leukocyte or macrophage populations. Mucosal MPO-positive cell populations were most commonly assigned grade 1, with occasional specimens given grades 2 or 3. There was an indication of increased numbers of neutrophils and macrophages in the jejunal mucosa of irradiated animals, but overt inflammation with marked inflammatory cell infiltration was not a feature of radiation injury to the jejunum.

CD3 immunohistochemical stain

Immunohistochemical staining for $CD3^+$ lymphocytes in the jejunum primarily involved mucosal cell populations, with occasional $CD3^+$ cells in the submucosa or within lymphoid follicles when those structures were fortuitously included in the jejunal sections. Most jejunal specimens had grade 2 mucosal populations of $CD3^+$ lymphocytes, with occasional specimens assigned grades 1 or 3. Lymphoid follicles were uncommonly included in the jejunal sections, therefore, the effect of irradiation on $CD3^+$ cell populations in jejunal lymphoid structures such as Peyer's patches could not be evaluated. The jejunal mucosa had no discernible variation in the population of $CD3^+$ cells relative to radiation dose or post-irradiation interval.

Bmi-1 immunohistochemical stain

Positive staining for Bmi-1 was noted in a subpopulation of epithelial cells located near the deep aspect of jejunal crypts, but typically not located in the bottom of crypts. The population of Bmi-1^+ cells was assigned grade 1 in the great majority of specimens. Subjective evaluation revealed no apparent alteration in the numerical density of the Bmi-1 cell population relative to radiation dose or post-exposure intervals.

IL22 immunohistochemical stain

A population of $IL22^+$ leukocytes was commonly present in the mucosa of the jejunal specimens from all treatment groups, including the naïve controls. There was evidence that the population of $IL22^+$ cells was influenced by the radiation level, as the jejunal specimens of 10 of 16 animals from the 12 Gy irradiation group had no discernible $IL22^+$ cell populations in the jejunal mucosa.

IL22R immunohistochemical stain

IL22R staining in jejunal epithelial cells was most commonly assigned grades of 2 or 3, with five specimens assigned a grade of 1 and three specimens assigned a grade of 4. Subjective evaluation revealed no discernible alteration in the population of IL22R expression in association with radiation level or post-irradiation interval.

Transforming growth factor β (TGFβ) immunohistochemical stain

Immunohistochemical staining for transforming growth factor-beta (TGFβ) was noted in the deep aspects of mucosal crypts of the jejunum, where it was co-located with Paneth cells. Neutrophils stained positively for TGFβ, thus served as an internal control for the technical

quality of the stains, but the neutrophil population was not considered in grade assignments. Positive TGFβ staining in crypts was most commonly graded as minimal or mild (grades 1 or 2, respectively), with occasional specimens graded as moderate (grade 3). Absent or low-level TGFβ staining in jejunal crypts was commonly associated with depletion and/or denudation of the mucosal epithelium, particularly in animals that were necropsied within 30 days of radiation exposure. By contrast, animals that were necropsied during the early post-irradiation period but had little microscopic evidence of mucosal epithelial depletion or denudation tended to have substantial levels of TGFβ staining in crypt epithelial cells.

Colon- (Figures 8a, 8b, 8c, 8d, 8e, 8f, 9a, 9b, 9c, 9d)

The routinely stained colon sections had a spectrum of histologic changes that were based on the same radiation-associated injury as that seen in the jejunum, but the histomorphologic manifestation in the colon was different because of the differences in normal histologic structure of the colon versus the jejunum. The colon has no villi, therefore, the striking contraction and loss of villi seen in the jejunum was not present in the colon. As in the jejunum, the most pronounced histologic changes in the colon were in animals irradiated at 12 Gy. The most common histologic alteration was epithelial depletion which, in its most advanced status, presented as mucosal denudation. The colonic changes were considered to be a major contributor to the shorter survival time of animals in this group. Similar but less pronounced histologic changes were present in animals irradiated at 10 or 11 Gy.

Inflammatory cell infiltration in the colon was notably sparse relative to the degree of epithelial disruption. This was presumed to be a result of radiation effects on the hematopoietic system.

Colonic fibrosis, as visualized with Masson's trichrome staining, was subcategorized as mucosal, submucosal or serosal. The subtle mucosal fibrosis was difficult to detect with Masson's trichrome staining, but increased mucosal collagen deposition was discernible with collagen immunohistochemical staining (see below). Submucosal and serosal fibrosis in the colon was sporadically observed, with more common occurrence in animals irradiated at 11 or 12 Gy. As with the jejunum, the fibrotic lesions in the colon tended to be focal or multifocal, which raised concerns that the somewhat sparse specimen collection for the jejunum and colon may have created a false impression of the true incidence of post-irradiation colonic fibrosis.

LPS core immunohistochemical stain- (Figure 9e)

Staining for lipopolysaccharide (LPS) core antigen was subcategorized as lamina propria or submucosal staining. One naïve control animal had a minimal (grade 1) number of LPS core-positive cells in the lamina propria, and another animal had mild (grade 2) LPS core^{+} cells in germinal centers of a small lymphoid follicle that was fortuitously included in the histologic sections of colon. Remaining naïve control animals had no LPS core IHC staining in the colonic mucosa. The irradiated animals commonly had LPS core^{+} cells in the lamina propria but, despite the obvious radiation-associated damage to the mucosa, only 2 animals had LPS core+ cells in the submucosa. LPS core^{+} bacteria were commonly present on the

mucosal surface, thus serving as an internal control for the immunohistochemical staining procedure.

MxA immunohistochemical stain- (Figure 9f)

Immunohistochemical staining for MxA was subcategorized as mucosal or submucosal staining. Mucosal staining for MxA was presented in all of the naïve control animals, and was assigned grade 1 in five animals and grade 2 in one animal. More pronounced MxA staining was present in the mucosa of many irradiated animals, but this effect appeared to dissipate somewhat during the course of the observation period. The increased populations of MxA^+ cells in the colonic lamina propria indicated the presence of activated immunocytes. It should be noted that the concurrent effects on the hematopoietic system and thymus would be expected to have a dampening effect on the population of activated immunocytes in the peripheral tissues.

Myeloperoxidase (MPO) immunohistochemical stain-

Immunohistochemical staining for MPO in colonic specimens was limited to mucosal staining, primarily indicating MPO^+ leukocyte or macrophage populations. MPO^+ cell populations in the colonic mucosa of naïve control animals were most commonly grade 1, with a single naïve control animal assigned grade 2. Grade 2 MPO^+ cell populations were observed in 21 animals irradiated at 11 or 12 Gy, and grade 3 MPO^+ cell populations were observed in two animals irradiated at 12 Gy and one animal irradiated at 11 Gy. The increased populations of MPO^+ cells were an indication of inflammatory reactions associated with radiation injury and secondary changes in the colon. It was interesting to note the study animal with the most pronounced neutrophilic infiltration in the colonic mucosa also had the most pronounced population of MPO^+ cells.

CD3 immunohistochemical stain

Immunohistochemical staining for $CD3^+$ lymphocytes in the colon primarily involved mucosal cell populations, with occasional $CD3^+$ cells in the submucosa or lymphoid follicles when those latter structures were fortuitously included in the jejunal sections. Most colonic specimens had a grade 2 mucosal population of $CD3^+$ lymphocytes, with little influence associated with radiation dose or post-exposure interval. Colonic lymphoid follicles commonly had pronounced reduction in lymphocyte populations, as an expected consequence of irradiation. Medical management of the irradiated animals included administration of dexamethasone, a known immunosuppressant that may have complicated interpretation of colonic lymphoid follicle changes in the later stages of the observation period.

CD13 immunohistochemical stain (Figure 10a)

Positive staining for CD13 in the colonic mucosa consisted of staining of individual cells, consistent with leukocytes or macrophages. Presence of a grade 1 population of $CD13^+$ cells in the colonic mucosa of naive control animals served as the basis for comparison for specimens from irradiated animals. Grade 2 or 3 populations of CD13+ cells in the colonic mucosa were associated with radiation injury or associated inflammatory reactions, as was

also demonstrated by the presence of myeloperoxidase$^+$ cells (see above). There was a trend toward early increases in CD13$^+$ cells in animals irradiated at 12 Gy, with later increases in animals irradiated at 11 or 10 Gy.

Collagen 1 immunohistochemical stain- (Figures 10b, 10c, 10d)

Increased collagen staining was subcategorized based on location in the mucosa, submucosa, muscularis externa, or serosa of the colonic specimens. The level of collagen staining observed in colonic specimens from the naive controls was used as a baseline (grade of 0) for the subjective determination of increased collagen staining in specimens from the irradiated animals. It appears the 12 Gy irradiation level may have reached a threshold for colonic fibrosis. Increased mucosal collagen staining was uncommonly noted in animals other than the group irradiated at 12 Gy, in which 7 of 15 animals had increased colonic mucosal collagen staining. Increased submucosal collagen staining was also noted in the colon of 4 of 15 animals irradiated at 12 Gy, and greatly increased collagen staining was noted in the muscularis externa of one animal that was irradiated at 12 Gy and survived to day 102 post-irradiation. Increased collagen staining was observed only sporadically in the colon of irradiated animals, but it should be noted that increased collagen staining in the various sublocations of the colon tended to be multifocally distributed. Only two specimens from the colon were examined microscopically, thus it is possible examination of a more extensive sample collection would reveal additional examples of increased collagen staining.

Transforming growth factor β (TGFβ) immunohistochemical stain

TGFβ staining was rarely noted in the mucosal lamina propria of the colon. When present, it appeared to be expressed by neutrophils and possibly macrophages. Subjective evaluation revealed no discernible alteration in TGFβ$^+$ cell populations as related to radiation dose or post-irradiation interval.

Connective tissue growth factor (CTGF) immunohistochemical stain- (Figures 10e, f)

Immunohistochemical for connective tissue growth factor (CTGF) staining was not noted in the colonic mucosa of the naïve control animals, but low-intensity staining was noted in the colonic specimens from irradiated animals, particularly animals irradiated at 12 GY. The grade 1 or grade 2 CTGF staining in the colon involved cells consistent with leukocytes or macrophages in the lamina propria, The low level of the stain intensity aroused suspicion of nonspecific staining, but the specimens from the naïve control animals had no evidence of the low-intensity staining.

Mast cell populations

Mast cells were present at minimal (grade 1) level in the colon of all naïve control animals. With toluidine blue staining, mast cells were essentially absent from the colon of 6 of 12 animals irradiated at 11 Gy and 9 of 16 animals irradiated at 12 Gy. With tryptase immunohistochemical staining, 9 of 16 animals irradiated at 12 Gy had the lowest level (grade 1) mast cell populations in the colon. These observations suggest radiation dose-related depletion of mast cells from the colonic mucosa, but the same technical

considerations mentioned above under jejunum should be applied to interpretation of mast cell populations in the colon.

Alpha smooth muscle actin immunohistochemical stain

Immunohistochemical staining for alpha smooth muscle actin (α-SMA) was subcategorized as mucosal, submucosal or serosal. The α-SMA staining generally paralleled the histologic evidence of fibrosis as recorded under the trichrome stains.

Bmi-1 immunohistochemical stain

The population of Bmi-1^+ cells in colonic crypts was graded as grade 1 in the majority of specimens, with specimens occasionally assigned grade 2. Subjective evaluation revealed no alteration in the population of Bmi-1+ cells relative to radiation dose or post-irradiation interval.

IL22 immunohistochemical stain

$IL22^+$ cells were inconsistently demonstrated in the colonic mucosa. There was no discernible difference in the population of IL22+ cells relative to radiation dose or post-irradiation interval.

IL22R immunohistochemical stain

IL22R staining was common in colonic epithelial cells, and was assigned grades 2, 3, or 4 in two each of the naïve control animals. Subjective evaluation revealed no indication of an alteration in IL22R expression in association with radiation dose or post-irradiation interval.

Periodic acid-Schiff/alcian blue (PAS/alcian blue) stain

The PAS/alcian blue stain revealed the mucin content of mature mucin-producing (goblet) cells in the colonic mucosa. The population of mature intestinal epithelial cells was markedly diminished as a result of radiation injury, thus the number of goblet cells was similarly diminished. The population of mature goblet cells was re-established with revitalization of the colonic epithelium. The PAS component of the dual stain resulted in magenta staining of goblet cell contents, while staining with the alcian blue component resulted in blue staining of goblet cell contents. Subjective evaluation revealed no discernible difference in PAS versus alcian blue staining of goblet cell mucin as associated with radiation dose or post-irradiation interval.

Mesenteric lymph node- (Figures 11a, 11b, 11c)

Lymphoid depletion was noted in a number of animals from all groups except the naïve control group. A modified enhanced immunohistopathology approach (Elmore 2012) was utilized, which included separate histologic grades being applied to the cellularity of follicles, germinal centers, paracortex and medullary cords. The summary observation of ‘lymphoid depletion’ integrated the various facets of the lymphoid changes on an animal-by-animal basis at the time the histopathologic evaluation was performed. It was interesting to note that grade 4 lymphoid depletion was present in the mesenteric lymph nodes of 8 of 14 animals irradiated at 12 Gy, and grade 5 in an additional animal from that group. It should be

noted that administration of corticosteroids such as dexamethasone is known to result in lymphoid depletion in lymph nodes, therefore, clinical supportive measures employed in the present study may have complicated lymphoid changes in the mesenteric lymph nodes. Dexamethasone was not administered to any animals prior to post-irradiation day 42, therefore, the lymphoid depletion noted in decedent animals in that time period was unequivocally due to radiation effects. Dexamethasone supportive therapy was commonly employed starting at approximately post-irradiation day 70, therefore, the incidence of lymphoid depletion from day 70 through the end of the observation period may have been influenced by dexamethasone therapy. The clinical records of nine animals had no indication of dexamethasone therapy, and none of those nine animals had histological evidence of lymphoid depletion in the mesenteric lymph nodes, suggesting dexamethasone therapy had some influence on lymphoid depletion in the mesenteric lymph node in the later stages of the observation period.

Marked bacterial invasion was noted in the mesenteric lymph node of one animal irradiated at 11 Gy. The identity of the bacterial species was not apparent from routine histopathologic examination, but the general features suggested the organisms were coccoid rather than the rod-shaped organisms typically encountered with coliform bacteria. Tissue gram stains revealed a mixed bacterial population, with a preponderance of gram-positive cocci.

Eosinophil infiltrations in mesenteric lymph nodes of a few animals were assigned no particular importance, as they were suspected to be associated with intestinal parasitism. Eosinophil infiltrations were also present in the mesenteric lymph nodes of 3/6 naïve control animals.

The Masson’s trichrome stains revealed minimal evidence of fibrosis in the mesenteric lymph nodes. See the section on collagen stains, which resulted in a more precise identification of fibrous connective tissue in the lymph nodes.

Mast cell populations

Mast cells as revealed by toluidine blue staining were essentially absent from the mesenteric lymph nodes. Tryptase staining revealed a slightly greater population of mast cells within mesenteric lymph nodes than were revealed by toluidine blue staining. This could reflect a population of intestinal mucosal mast cells that translocated to the mesenteric lymph nodes, and were not revealed by toluidine blue staining. Mast cell populations were recorded only in the parenchyma of the mesenteric lymph nodes, and did not include minor mast cell populations in connective tissue surrounding the lymph nodes. There was no discernible alteration in mast cell populations as related to radiation dose or post-irradiation interval.

Tryptase immunoreactivity was noted on the surface of sinusoidal macrophages in irradiated animals (Figures 11d, 11e, 11f). The genesis and significance of this observation are unknown. Macrophage tryptase staining was not observed in mesenteric lymph nodes of the naïve control animals, thus it is likely the macrophage tryptase reactivity was in some way related to irradiation. Given the evidence of radiation effects on mast cell populations in the current study and reported in the literature, it is possible the tryptase immunostaining on the

surface of sinusoidal macrophages in the mesenteric lymph nodes represented sequestration of tryptase enzymes released from intestinal mast cells.

Alpha smooth muscle actin immunohistochemical stain

There was little evidence of α-SMA staining in the mesenteric lymph nodes.

MxA immunohistochemical stain- (Figures 12a, 12b, 12c, 12d, 12e)

Staining for MxA was subcategorized based on location in the subcapsular sinuses or medullary region. Subcapsular MxA staining was not present in naïve control animals, but grade 1 or grade 2 MxA staining was present in the medullary region of the mesenteric lymph nodes of all naïve control animals. Clusters of MxA+ cells were also observed in the germinal centers of two naïve control animals, indicating the presence of activated immune cells in germinal centers and medullary compartments are part of normal immune system homeostasis. By contrast, subcapsular sinuses of many of the irradiated animals contained MxA-positive cells, the histologic features of which were consistent with macrophages or dendritic cells. Presence of the MxA-positive cells in subcapsular sinuses of mesenteric lymph nodes was considered to be evidence of immunologic reactions in the intestines.

LPS core immunohistochemical stain

Staining for LPS core antigen was subcategorized as cortical, germinal center, medullary, or subcapsular sinus staining. The naïve control animals had evidence of LPS core-positive cells in each of these sub-locations, with severity grades similar to those seen in irradiated animals. The mesenteric lymph node appeared to serve as a collecting vessel for LPS core-positive cells that were migrating from upstream sites in the intestine. The present study revealed no histological evidence, based on subjective evaluation, that there was a radiation-associated increase in the rate of delivery or internal processing of LPS core antigen in the mesenteric lymph nodes.

Myeloperoxidase (MPO) immunohistochemical stain- (Figures 13a, 13b, 13c, 13d, 13e)

Myeloperoxidase staining in the mesenteric lymph node was subcategorized as medullary or subcapsular sinus, based on the location of the positively stained cells. Positively stained cells were considered to be primarily macrophages/histiocytes or neutrophils, based on the size and nuclear profile of the cells. Positive MPO staining of cells in the subcapsular sinuses was not present in naïve control animals, but was observed in low incidence among irradiated animals. MPO^+ cells in subcapsular sinuses were most commonly observed in animals irradiated at 12 Gy, only two of which survived beyond 30 days. MPO-positive cells in subcapsular sinuses were noted at a lower incidence rate in animals irradiated at 11 Gy, and were not observed in animals irradiated at 10 Gy. Migratory cells in subcapsular sinuses of mesenteric lymph nodes typically originate from pathologic processes in the intestine, thus it is assumed the subcapsular MPO^+ cell population observed in the mesenteric lymph nodes was a reflection of radiation-associated intestinal injury. The medullary MPO staining was most commonly graded as grade 1, as applied to 5 naïve control animals, or grade 2, as applied to 1 naïve control animal, but in 8 irradiated animals the medullary MPO staining was graded as grade 3 or grade 4.

Collagen 1 immunohistochemical stain- (Figures 14a, 14b, 14c, 14d)

The histopathology data entries of positive collagen staining in the mesenteric lymph nodes refer to collagen deposits other than the normal collagenous tissue that surrounds blood vessels in the hilus and medulla of the lymph nodes. In essence, these entries represent collagen deposition in the cortex of the lymph nodes. Increased collagen deposition was noted in the mesenteric lymph nodes of 6 of 30 animals irradiated at 10 Gy, 9 of 43 animals irradiated at 11 Gy, and 4 of 17 animals irradiated at 12 Gy, suggesting no dose-related influence on the incidence of collagen deposition in the mesenteric lymph nodes. However, it is likely the apparent absence of a radiation dose response in the present study was influenced by the short survival time of animals in the 12 Gy irradiation group. Only two animals irradiated at 12 Gy survived beyond 30 days, and none survived beyond 102 days.

Transforming growth factor β (TGFβ) immunohistochemical stain- (Figures 15a, 15b, 15c)

Transforming growth factor-beta (TGFβ) staining was subcategorized as subcapsular sinus or medullary staining, based on the location of positively stained cells within the mesenteric lymph node. Grade 2 medullary TGFβ staining was noted in 1 naïve control animal, but the subcapsular sinuses and medullary regions of mesenteric lymph nodes of the remaining naïve control animals were devoid of TGFβ staining. TGFβ staining of cells in the subcapsular sinuses and medullary regions of irradiated animals was more commonly observed during the first 30 days following irradiation, and was most commonly noted in animals irradiated at 12 Gy. Of the 15 animals irradiated at 12 Gy and necropsied before post-irradiation day 30, five had TGFβ expression in the medullary region of the mesenteric lymph node, and an additional four animals had TGFβ expression in both the medullary region and subcapsular sinuses. As noted above, there appeared to be a relationship between TGFβ and CTGF expression and collagen deposition.

Connective tissue growth factor (CTGF) immunohistochemical stain- (Figure 15d)

Positive staining for connective tissue growth factor (CTGF) was subcategorized as subcapsular sinus, cortical or medullary staining, based on the location of positively stained cells within the mesenteric lymph node. CTGF staining was not observed in mesenteric lymph nodes of the naïve control animals, but was observed in the cortex, medulla and subcapsular sinuses of a small number of irradiated animals. CTGF expression in the mesenteric lymph nodes was most commonly observed in animals necropsied during the first 50 days following irradiation, and was more commonly observed in animals irradiated at 11 and 12 Gy. Four animals with positive CTGF staining had concurrent collagen 1 staining, while seven animals with CTGF staining had no staining for collagen 1. There was slightly greater evidence for a relationship between CTGF staining and TGFβ staining, as seven animals with CTGF staining had concurrent TGFβ staining, while only four animals with CTGF staining did not have TGFβ staining. When the 15 irradiated animals with demonstrated increases in collagen 1 deposition in the mesenteric lymph node are considered, it was noted that seven had TGFβ staining, two had CTGF staining, and two had staining for both TGFβ and CTGF. These observations suggest relationships between lymph node collagen deposition and expression of TGFβ and CTGF. It should be noted that these

processes and signaling events probably exist in a sequence, therefore, it may be unreasonable to expect all the markers to be expressed in the same lymph node.

DISCUSSION

A more detailed description of the immediate post-irradiation intestinal response was recently published (Macvittie et al. 2018), thus is not replicated here. The post-irradiation responses of the intestinal mucosa are well-known, and considered to be due to failure in replication of rapidly dividing intestinal crypt cells subsequent to radiation damage to nucleic acids. Within a few days the surviving animals developed niches of proliferative cells within preexisting crypts. The proliferative epithelial cells eventually reconstituted the mucosal epithelium, complete with formation of villi. However, repair of the radiation-associated mucosal injury was imperfect, as evidenced by zones of depleted epithelial cells, villus blunting and villus fusion in animals necropsied throughout the observation period.

Pronounced fibrosis, located most commonly in the submucosa and serosal surface, was observed in a subset of animals. The submucosal and serosal fibrosis tended to be focal or multifocal within the intestinal sections, thus raising concerns that the modest intestinal sampling (two specimens each of colon and jejunum) may not have revealed the true incidence of intestinal fibrosis. Localization of the fibrogenic process in the submucosa and serosa was interesting, but unexplained. The submucosa is closely approximated to the mucosa, thus it is reasonable to suspect the submucosal lesions represent an extension of mucosal injury. However, the serosal surface is separated from the mucosa by the muscularis mucosa, submucosa and two thick layers of muscularis externa. It is difficult to visualize how a radiation-associated alteration in the mucosa could result in fibroplasia in the serosa as a result of direct extension of the mucosal lesion. Observations in the present study suggest the intestinal fibrosis was due to a primary fibrogenic effect of irradiation upon unspecified cell populations in the submucosa and serosa, as opposed to a simple extension of a mucosal lesion into other layers of the intestine. This suspicion was augmented by specific observations in the present study, including an extensive population of reactive, fibrogenic cells in the submucosa of an animal (see figures 2a and 2b) that had only grade 2 epithelial cell depletion in the overlying mucosa and an intact mucularis mucosa separating the mucosa from the submucosa.

A comparatively minor element of collagen deposition, as indicated by immunhistochemical staining, was occasionally observed in the jejunal and colonic mucosa, but was not a consistent finding. Localization of the mucosal collagen deposition in the specific site of the previous radiation-associated mucosal injury suggests the collagen deposition was post-injury fibrogenesis, as is seen with the general process of scar tissue formation in other organs. The mucosal collagen deposition was not of a striking magnitude from a histological perspective, but it could nonetheless have a significant impact on overall function of the intestinal mucosa.

Despite the degree of mucosal injury, inflammatory cell infiltration was not a prominent feature of the intestinal response to irradiation. In all probability the degree of inflammatory cell infiltration was dampened by radiation-associated depletion of bone marrow

hematopoietic reserves, which would be expected to reduce hematopoietic responsiveness despite the marrow preservation technique employed in the present study.

There is evidence that mast cell populations in the intestine are altered by radiation exposure (Richter et al. 1997, Zheng et al. 2000, Wang et al. 2014), therefore, mast cell populations were investigated in the present study. There was evidence that intestinal mast cell populations were reduced immediately following irradiation, particularly in animals irradiated at 12 Gy. This effect was observed only upon staining with toluidine blue, and not when the intestinal sections were subjected to immunohistochemical staining for tryptase. The toluidine blue staining is known to reveal only the connective tissue mast cell population, and does not include the mucosal mast cell population unless special fixatives are used at the time of tissue collection (Enerback 1966, Strobel et al. 1981, Wingren and Enerback 1983, Enerback 1987). The somewhat sparse observations in the present study cannot be interpreted as conclusive, but suggest irradiation may have an immediate effect on the connective tissue mast cell population but not the mucosal mast cell population. The present study had no indication that increased mast cell populations were involved in the late effects of radiation injury to the intestine.

As documented by numerous previous observations, the mesenteric lymph nodes of irradiated rhesus macaques consistently had lymphoid changes associated with radiation injury to lymphoid cell populations. In the present study, radiation-associated lymphoid effects that were unequivocally attributable to irradiation could be determined only in animals necropsied before day 42 post-irradiation. After that time, histological interpretation of lymphoid changes in mesenteric lymph nodes may have been complicated by the corticosteroid administration that was part of the medical management program.

A number of lymph node alterations were considered to be secondary to intestinal alterations. Mesenteric lymph nodes of irradiated animals contained an increased number of activated immunocytes, as demonstrated by positive MxA immunohistochemical staining. MxA^+ cells were commonly present in subcapsular sinuses of mesenteric lymph nodes, suggesting the cells were migrating from the intestine. Mesenteric lymph nodes of irradiated animals had higher incidence and/or severity of cells staining positively for lipopolysaccharide (LPS) core, suggesting accumulation of LPS-containing cells that were migrating from the injured intestine. There was an increase in the number of MPO^+ cells, consistent with neutrophils and reactive macrophages, in the mesenteric lymph nodes of a subset of irradiated animals. Presence of MPO^+ cells in the mesenteric lymph node was related to level of irradiation, presumably reflecting the greater degree of intestinal mucosal injury with higher levels of irradiation. Tryptase staining of lymph nodes from irradiated animals, but not naïve control animals, commonly revealed $tryptase^+$ cells in subcapsular sinuses. The tryptase staining was typically located at the cell surface, suggesting accumulation of $tryptase^+$ material on the surface of the cells. Degranulation of intestinal mast cells was considered a likely source of the $tryptase^+$ material in/on subcapsular sinus cells in the mesenteric lymph nodes. Bacterial colonization was occasionally noted in mesenteric lymph nodes, but bacterial invasion was not a common feature of the mesenteric lymph node response. Likewise, there was little evidence of overt inflammation in the mesenteric lymph nodes.

While the incidence and severity of fibrosis in the mesenteric lymph nodes was low, the potential impact of the fibrosis on overall lymph node function may be disproportionately significant. In addition to the plethora of biochemical and physiological events that take place in lymph nodes, there is an additional requirement for orchestrated movement of lymphoid cells through the various compartments of the lymph node in order for effective immunity to be instituted. These movements are controlled to a major degree by the placement and function of fibroblastic reticular cells (FRCs) in lymph nodes (Link et al. 2007, Fletcher et al. 2015). Though the degree of fibrosis seen in mesenteric lymph nodes in the present study did not appear overwhelmingly significant from a histopathological perspective, it is possible a relatively minor amount of collagen deposition could have a major influence on overall immunological function of the lymph node.

Transforming growth factor-beta (TGFβ) and connective tissue growth factor (CTGF) are known to have major roles in the generation of fibrosis in multiple organs (Ito et al. 1998, Pan et al. 2001, Flanders 2004, Akhurst and Hata 2012, Zhang et al. 2015). However, as presented in companion articles (Parker et al. 2018, Parker et al. 2018), the expression of these molecules was not prominent in the lung and kidney of rhesus macaques that developed a substantial level of pulmonary and/or renal fibrosis following irradiation. By contrast, there was evidence that TGFβ and CTGF were involved in the collagen deposition observed in the mesenteric lymph nodes of the present study, suggesting the fibrogenesis noted in the mesenteric lymph nodes may have had a different pathogenesis than that observed in the lung, kidney, intestinal serosa and intestinal submucosa.

Acknowledgments

This project has been funded in whole or in part with Federal funds from the National Institute of Allergy and Infectious Diseases, National Institutes of Health, Department of Health and Human Services, under Contracts HHSN272201000046C and HHSN272201500013I.

REFERENCES

Akhurst RJ, Hata A. Targeting the tgfbeta signalling pathway in disease. Nature reviews Drug discovery 11: 790–811; 2012. [PubMed: 23000686]

Bancroft JD, Stevens A. Theory and practice of histological techniques 4 ed. New York: Churchill Livingston; 1996.

Carson FL. Histotechnology- a self-instructional text Chicago: ASCP Press; 1997.

Elmore SA. Enhanced histopathology of the immune system: A review and update. Toxicologic pathology 40: 148–56; 2012. [PubMed: 22089843]

Enerback L Mast cells in rat gastrointestinal mucosa. I. Effects of fixation. Acta Pathol Microbiol Scand 66: 289–302; 1966. [PubMed: 4162017]

Enerback L Mucosal mast cells in the rat and in man. International archives of allergy and applied immunology 82: 249–55; 1987. [PubMed: 2437041]

Flanders KC. Smad3 as a mediator of the fibrotic response. Int J Exp Pathol 85: 47–64; 2004. [PubMed: 15154911]

Fletcher AL, Acton SE, Knoblich K. Lymph node fibroblastic reticular cells in health and disease. Nature reviews Immunology 15: 350–61; 2015.

Ito Y, Aten J, Bende RJ, Oemar BS, Rabelink TJ, Weening JJ, Goldschmeding R. Expression of connective tissue growth factor in human renal fibrosis. Kidney international 53: 853–61; 1998. [PubMed: 9551391]

Lendrum AC. The phloxine-tartrazine method as a general histological stain for demonstration of inclusion bodies. J Pathol Bacteriol 59: 399–404; 1947.

Link A, Vogt TK, Favre S, Britschgi MR, Acha-Orbea H, Hinz B, Cyster JG, Luther SA. Fibroblastic reticular cells in lymph nodes regulate the homeostasis of naive t cells. Nature immunology 8: 1255–65; 2007. [PubMed: 17893676]

Macvittie T, Farese A, Parker G, Jackson W, Booth C, Tudor G, Hankey K. The gastrointestinal syndrome of the acute radiation syndrome in rhesus macaques: A systematic review of the lethal dose response relationship with and without medical management Health physics: in press; 2018.

MacVittie TJ, Bennett A, Booth C, Garofalo M, Tudor G, Ward A, Shea-Donohue T, Gelfond D, McFarland E, Jackson W, 3rd, Lu W, Farese AM The prolonged gastrointestinal syndrome in rhesus macaques: The relationship between gastrointestinal, hematopoietic, and delayed multi-organ sequelae following acute, potentially lethal, partial-body irradiation. Health physics 103: 427–53; 2012. [PubMed: 22929471]

MacVittie TJ, Farese AM, Bennett A, Gelfond D, Shea-Donohue T, Tudor G, Booth C, McFarland E, Jackson W, 3rd. The acute gastrointestinal subsyndrome of the acute radiation syndrome: A rhesus macaque model. Health physics 103: 411–26; 2012. [PubMed: 22929470]

Pan LH, Yamauchi K, Uzuki M, Nakanishi T, Takigawa M, Inoue H, Sawai T. Type ii alveolar epithelial cells and interstitial fibroblasts express connective tissue growth factor in ipf. Eur Respir J 17: 1220–7; 2001. [PubMed: 11491168]

Parker G, Cohen E, Li N, Takayama K, Farese A, Macvittie T. Radiation nephropathy in a nonhuman primate model of partial-body irradiation with minimal bone marrow sparing. Part 2 of 2: Histopathology, mediators, and mechanisms. Health physics: in prep; 2018.

Parker G, Li N, Takayama K, Farese A, Macvittie T. Lung and heart injury in a nonhuman primate model of partial-body irradiation with minimal bone marrow sparing. Part 2 of 2: Histopathological evidence of lung and heart injury. Health physics: in prep; 2018.

Richter KK, Langberg CW, Sung CC, Hauer-Jensen M. Increased transforming growth factor beta (tgf-beta) immunoreactivity is independently associated with chronic injury in both consequential and primary radiation enteropathy. Int J Radiat Oncol Biol Phys 39: 187–95; 1997. [PubMed: 9300754]

Salzman NH. Paneth cell defensins and the regulation of the microbiome: Detente at mucosal surfaces. Gut Microbes 1: 401–6; 2010. [PubMed: 21468224]

Sheehan DC, Hrapchak BB. Theory and practice of histotechnology Columbus, OH: Battelle Press; 1980.

Strobel S, Miller HR, Ferguson A. Human intestinal mucosal mast cells: Evaluation of fixation and staining techniques. J Clin Pathol 34: 851–8; 1981. [PubMed: 6168659]

Wang J, Zheng J, Kulkarni A, Wang W, Garg S, Prather PL, Hauer-Jensen M. Palmitoylethanolamide regulates development of intestinal radiation injury in a mast cell-dependent manner. Digestive diseases and sciences 59: 2693–703; 2014. [PubMed: 24848354]

Wingren U, Enerback L. Mucosal mast cells of the rat intestine: A re-evaluation of fixation and staining properties, with special reference to protein blocking and solubility of the granular glycosaminoglycan. Histochem J 15: 571–82; 1983. [PubMed: 6192115]

Zhang P, Cui W, Hankey KG, Gibbs AM, Smith CP, Taylor-Howell C, Kearney SR, MacVittie TJ. Increased expression of connective tissue growth factor (ctgf) in multiple organs after exposure of non-human primates (nhp) to lethal doses of radiation. Health physics 109: 374–90; 2015. [PubMed: 26425899]

Zheng H, Wang J, Hauer-Jensen M. Role of mast cells in early and delayed radiation injury in rat intestine. Radiation research 153: 533–9; 2000. [PubMed: 10790274]

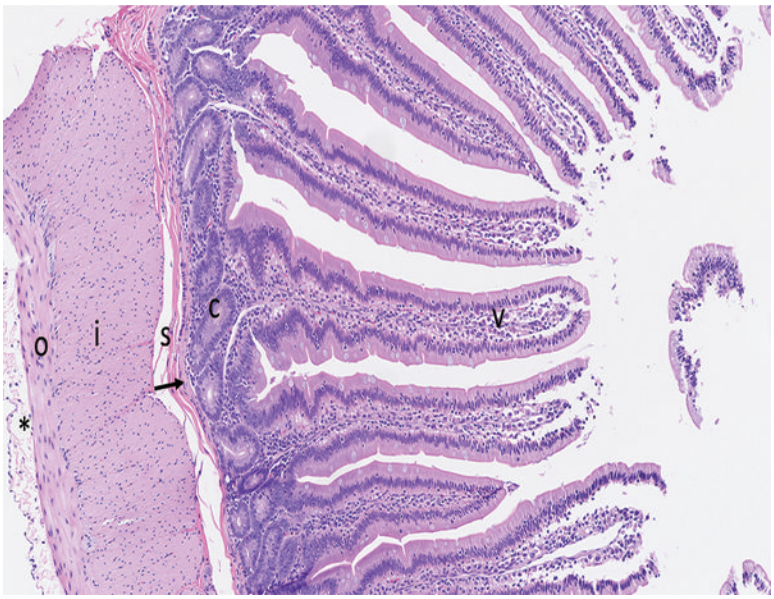

Figure 1a.

The histologic section of microscopically normal jejunum from an adult male rhesus macaque has elongated, finger-shaped villi (V) covered by an uninterrupted layer of columnar epithelial cells, and crypts (C) containing proliferative cells that replenish the superficial epithelial cells as they migrate up the villus and are eventually lost into the intestinal lumen. The muscularis mucosa (arrow) is a thin layer of smooth muscle that separates the mucosa from the underlying submucosa (s). The external muscular layer (‘muscularis externa’), divided into outer longitudinal (o) and inner circular (i) layers, serves to propel ingesta through the intestine via the process of peristalsis. The serosa (*) is thin and contains a sparse amount of fibrillar collagen. The loose connective tissue (‘lamina propria’) in the center of villi and surrounding the crypts contains a moderate number of leukocytes, including lymphocytes, macrophages, and occasionally a small number of neutrophils and eosinophils. The superficial epithelial layer of villi contains widely spaced leukocytes that are predominately T cells. Note the overall length of the villi, and the relative ratio of villus length to crypt depth. Fragments of villus epithelium in the intestinal lumen at the right side of the image are a result of tissue handling during specimen collection and gross trimming. H&E stain, 10x objective magnification.

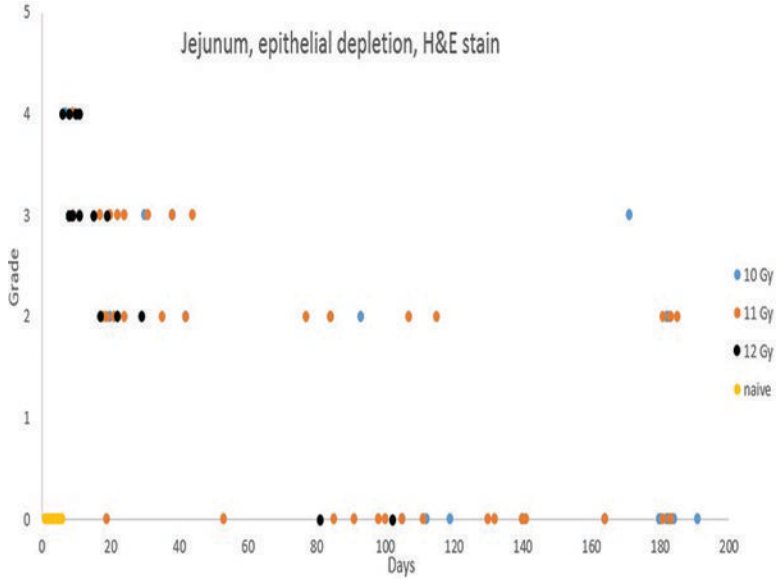

Figure 1b.

Depletion of mucosal epithelial cells was most prominent in the 40 days immediately following irradiation, but was noted to some degree in animals throughout the observation period. Epithelial depletion was more common and more pronounced in animals irradiated at 11 or 12 Gy.

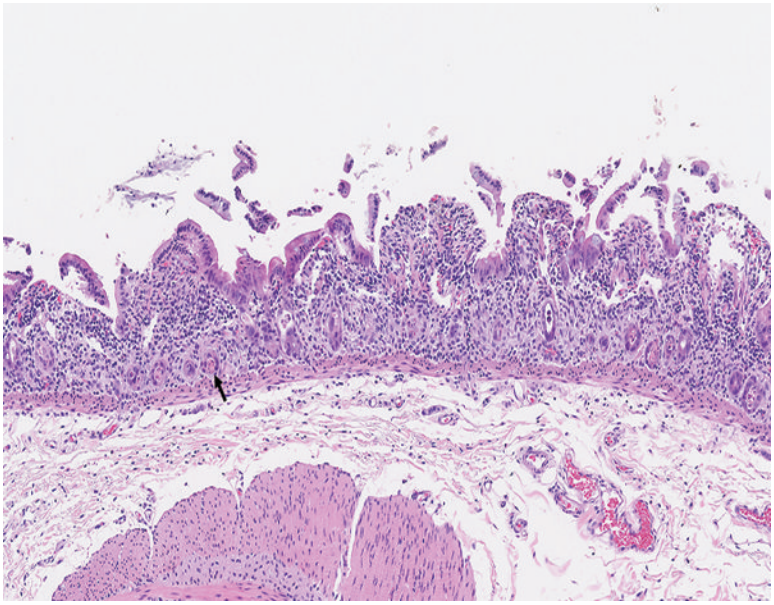

Figure 1c.

The jejunum of a male rhesus macaque collected at day 6 following irradiation at 12 Gy has markedly shortened villi. The luminal surface covered by attenuated epithelial cells, some of which are being lost as cellular rafts into the intestinal lumen. Few cellular elements remain in crypts (arrow). The leukocyte population in the lamina propria appears somewhat more prominent than in the normal jejunum, but some of this appearance may be due to contraction of the intestinal mucosa that results in visual concentration of pre-existing leukocytes. H&E stain, 10x objective magnification.

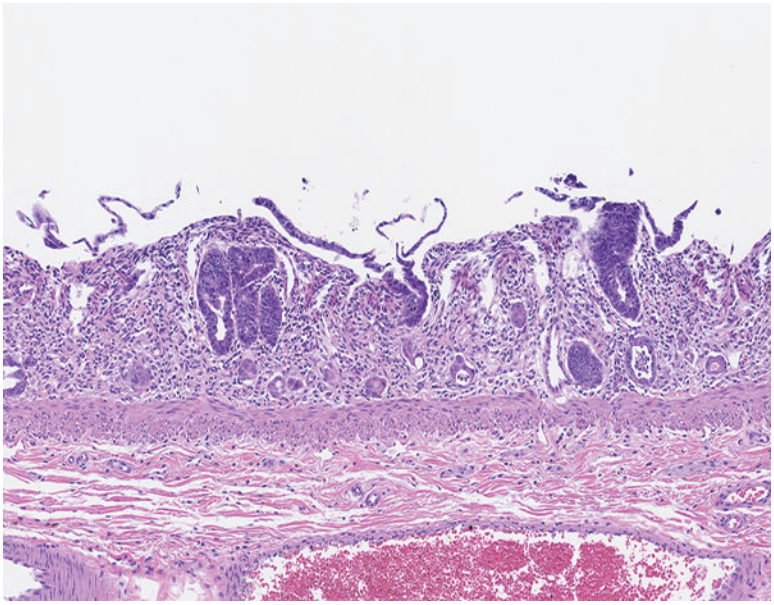

Figure 1d.

The jejunum of a male rhesus macaque collected at day 7 following irradiation at 10 Gy has no discernible villi, but multiple crypts are filled with deeply basophilic proliferative epithelial cells. Compare this image to the following image from an animal exposed to 12 Gy irradiation and necropsied on day 8. This comparison suggests crypt epithelial recovery was established sooner in animals that received the lower irradiation dose. H&E stain, 10x objective magnification.

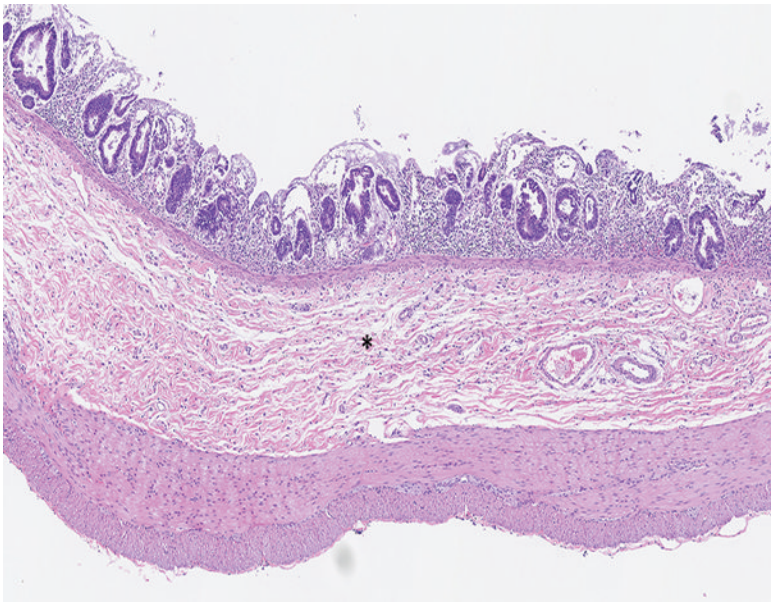

Figure 1e.

The jejunum of a male rhesus macaque collected at day 11 following irradiation at 10 Gy has an increased number of densely stained regenerative crypts and thickened submucosa (*). The luminal surface of the intestine remains devoid of intact villi. H&E stain, 5x objective magnification.

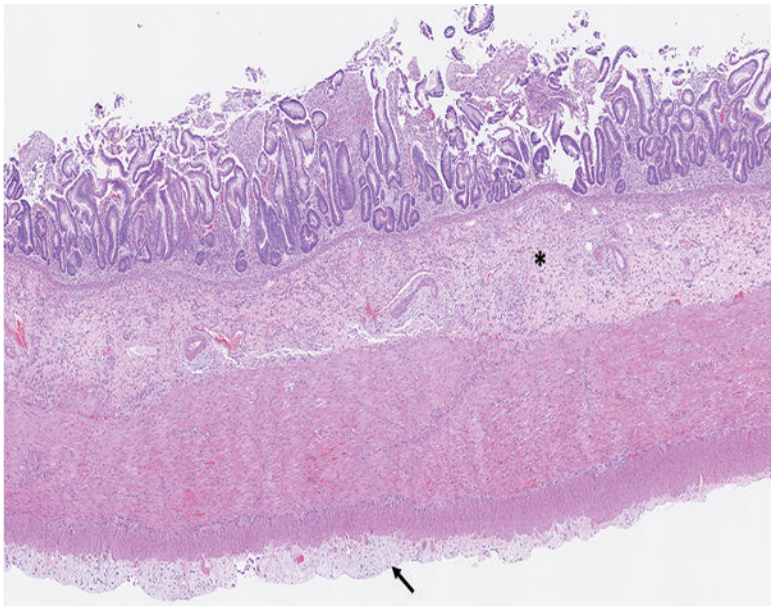

Figure 2a.

The jejunum of a male rhesus macaque collected at day 20 following irradiation at 10 Gy has transmural radiation-associated changes. The mucosal surface is devoid of intact villi, the submucosa (*) is thickened and hypercellular, and the serosa (arrow) has a plaque-like thickened zone. H&E stain, 2.5x objective magnification.

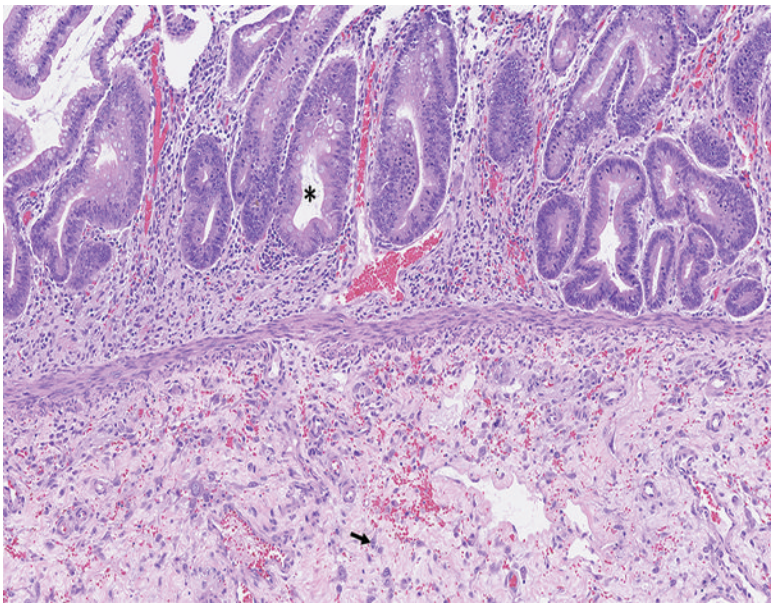

Figure 2b.

The higher magnification of jejunum of a male rhesus macaque collected at day 20 following irradiation at 10 Gy reveals regenerative crypts (*) with submucosal edema (light pink-stained material), and extravasated erythrocytes (red particles). The submucosa has numerous large mononuclear cells (arrow) that are consistent with active fibroblasts or myofibroblasts. H&E stain, 10x objective magnification.

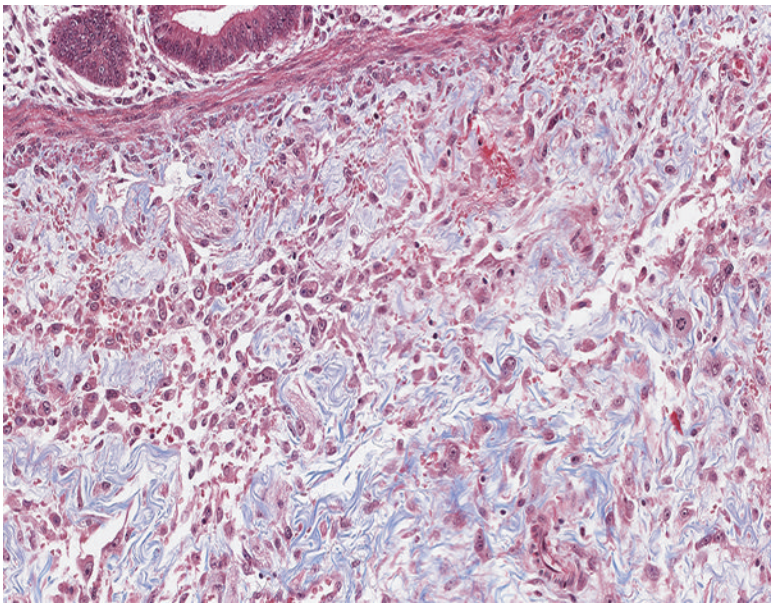

Figure 2c.

The jejunum of a male rhesus macaque collected at day 20 following irradiation at 12 Gy has blue-stained collagen fibrils in the submucosa as well as a substantial population of large mononuclear cells that are consistent with activated fibroblasts or myofibroblasts. Masson's trichrome stain, 20x objective magnification.

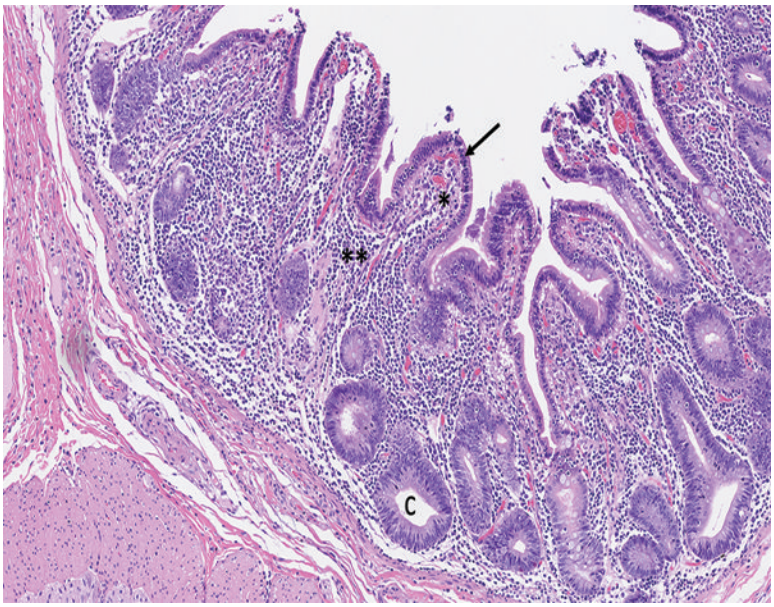

Figure 2d.

The jejunum of a male rhesus macaque collected at day 35 following irradiation at 11 Gy has short, blunt villi (*) that are covered by an intact layer of epithelial cells. The mucosal lamina propria (**) has a pronounced inflammatory cell population that consists primarily of lymphocytes. Crypts (c) remain in a highly proliferative status. H&E stain, 10x objective magnification.

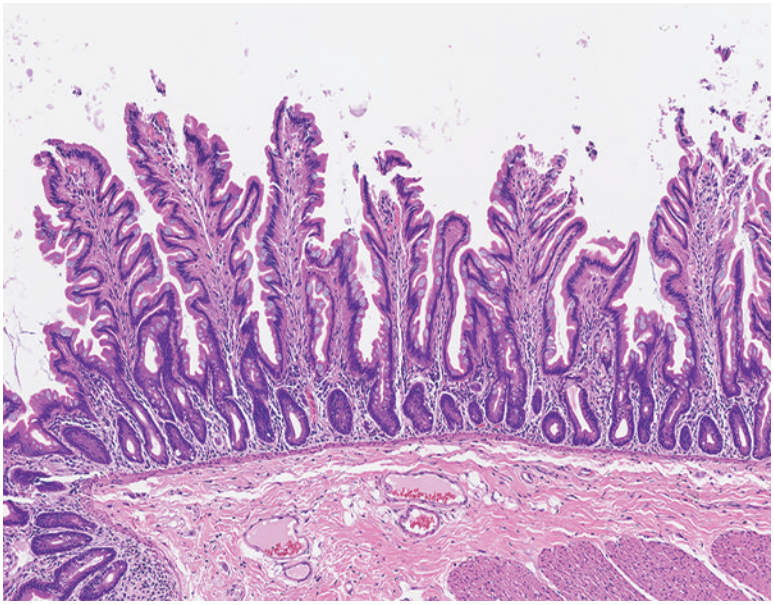

Figure 2e.

The jejunum of a male rhesus macaque collected at day 53 following irradiation at 11 Gy has numerous long villi that have a branching contour (‘leaf-shaped villi’), as opposed to the finger-shaped villi that are typical of intestinal mucosa of nonhuman primates. Leaf-shaped villi are occasionally present in the small intestine of ostensibly normal nonhuman primates, but an increased population of leaf-shaped villi has been associated with parenteral nutrition in humans. Leaf-shaped villi, thought to be a morphologic manifestation of mucosal atrophy, have an altered ratio of villus epithelial cells versus crypt epithelial cells. The leukocyte population in the lamina propria is equivalent to that seen in normal animals. H&E stain, 10x objective magnification.

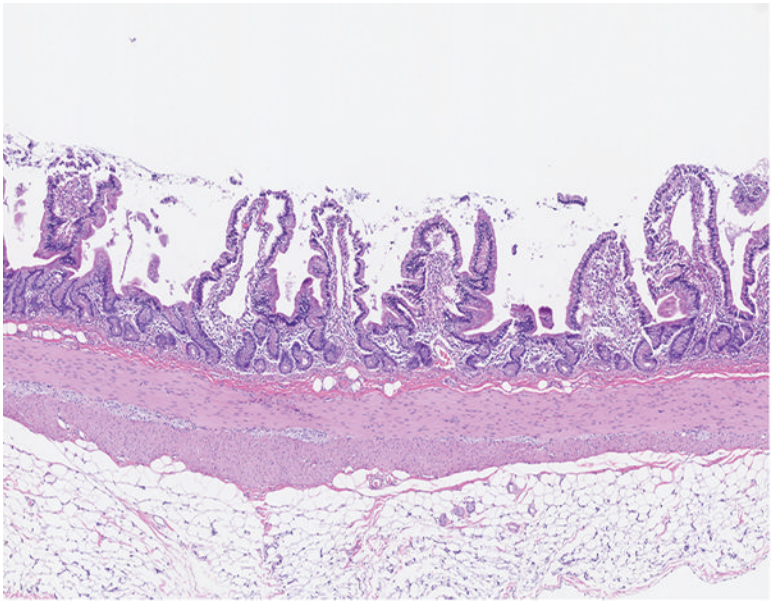

Figure 3a.

The jejunum of a male rhesus macaque collected at day 93 following irradiation at 10 Gy group has shortened, blunted villi and multiple expanses of mucosal surface that are devoid of villi. The leukocytic population in the lamina propria is equivalent to that seen in normal animals. H&E stain, 5x objective magnification.

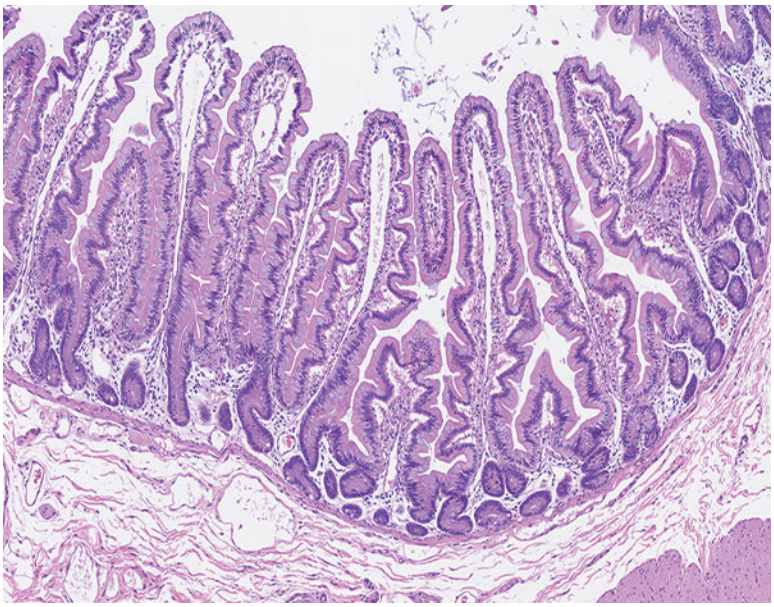

Figure 3b.

The jejunum of a male rhesus macaque collected at day 171 following irradiation at 10 Gy has completely regenerated villi with normal-appearing crypts, but many villi have irregular surface contour (‘leaf-shaped villi’), which is known to be associated with reduced intestinal functioning. H&E stain, 8.08x objective magnification.

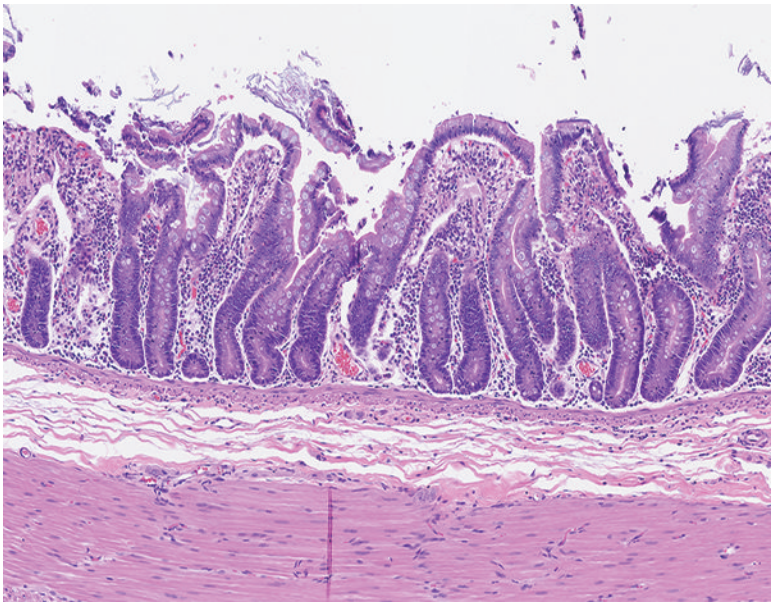

Figure 3c.

The jejunum of a male rhesus macaque collected at day 181 following irradiation at 11 Gy has shortened, fused villi and altered ratio of villus length to crypt depth. H&E stain, 10x objective magnification.

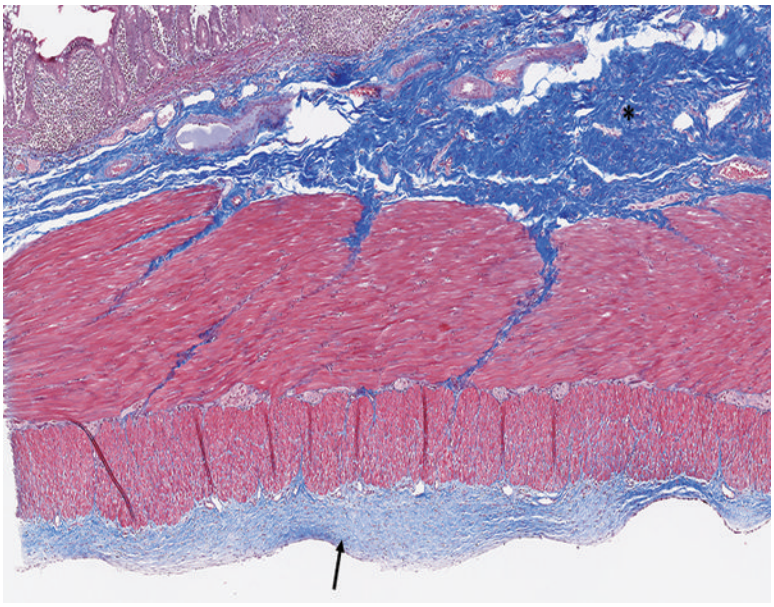

Figure 3d.

The jejunum of a male rhesus macaque collected at day 183 following irradiation at 11 Gy has an extensive area of blue-stained fibrous connective tissue in the submucosa (*) and a thick layer of fibrous tissue on the serosal surface (arrow). Masson's trichrome stain, 5x objective magnification.

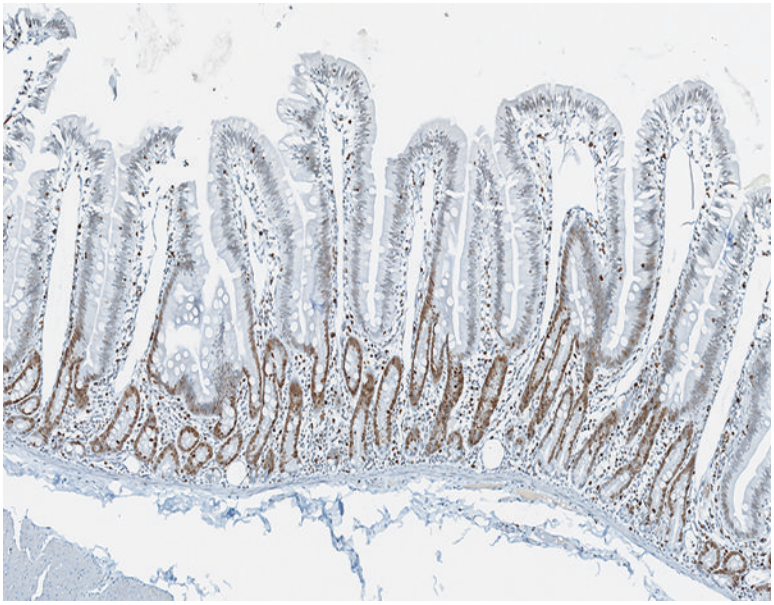

Figure 4a.

The jejunum of a naïve adult male rhesus macaque has extensive brown staining of proliferative crypt epithelial cells. Note the absence of proliferative cells on villi. Ki67 IHC stain, 10x objective magnification.

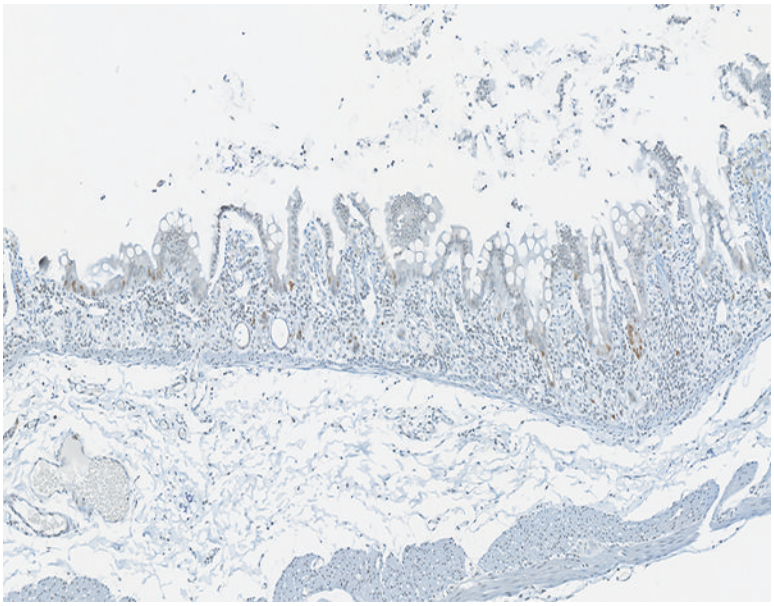

Figure 4b.

The jejunum of a male rhesus macaque collected at day 6 following irradiation at 12 Gy has short, blunted villi with sparse evidence of brown-stained crypt cell proliferation. Ki67 IHC stain, 10x objective magnification.

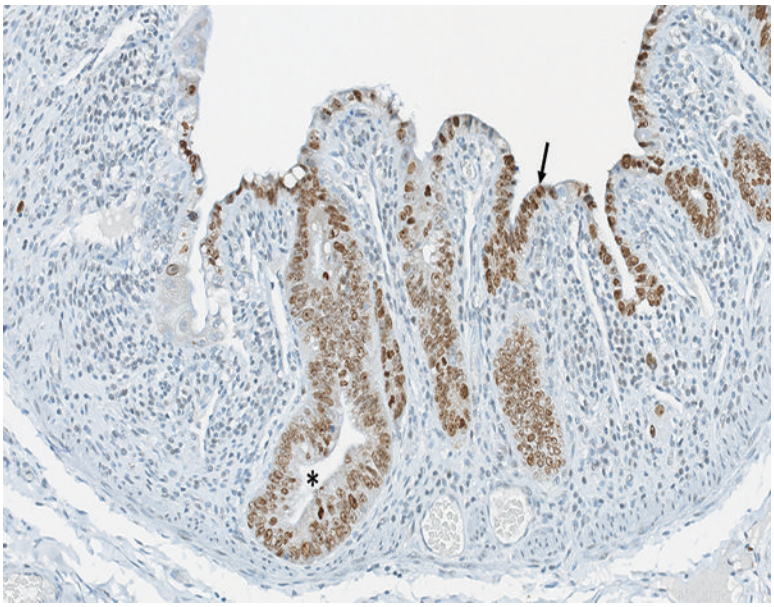

Figure 4c.

The jejunum of a male rhesus macaque collected at day 10 following irradiation at 12 Gy has extensive proliferative activity in crypts (*) and extending onto the luminal surface of what will become regenerating villi (arrow). Ki67 IHC stain, 20x objective magnification.

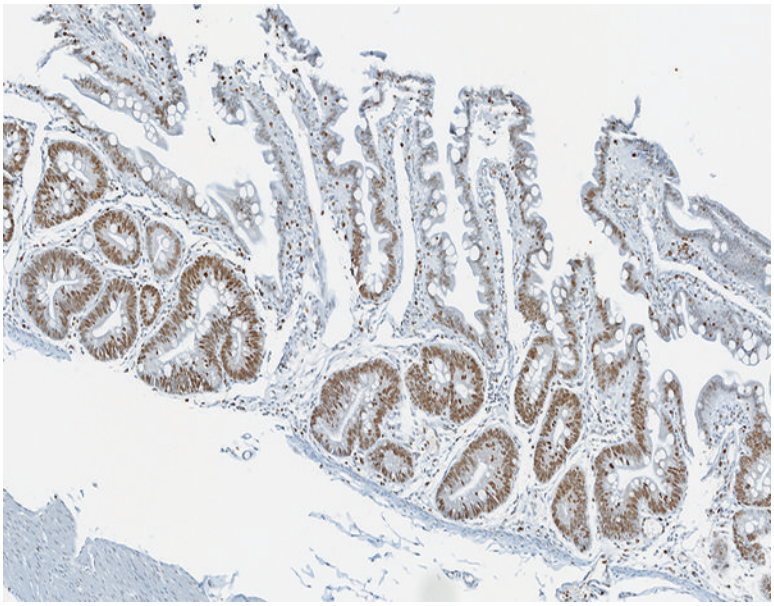

Figure 4d.

The jejunum of a male rhesus macaque collected at day 29 following irradiation at 12 Gy has extensive cellular proliferation within crypts. Presence of $Ki67^{+}$ cells extending up along the lateral edges of villi suggests an increased rate of migration of proliferative crypt cells, as compared to naïve controls. Ki67 IHC stain, 10x objective magnification.

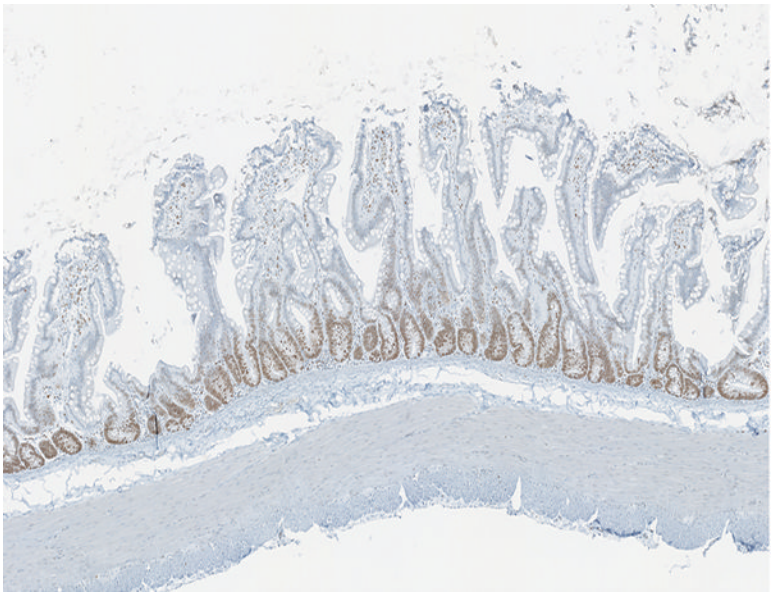

Figure 4e.

The jejunum of a male rhesus macaque collected at day 77 following irradiation at 11 Gy has the normal level of proliferative crypt cells, but villi are essentially devoid of proliferative cells. Ki67 IHC stain, 5x objective magnification.

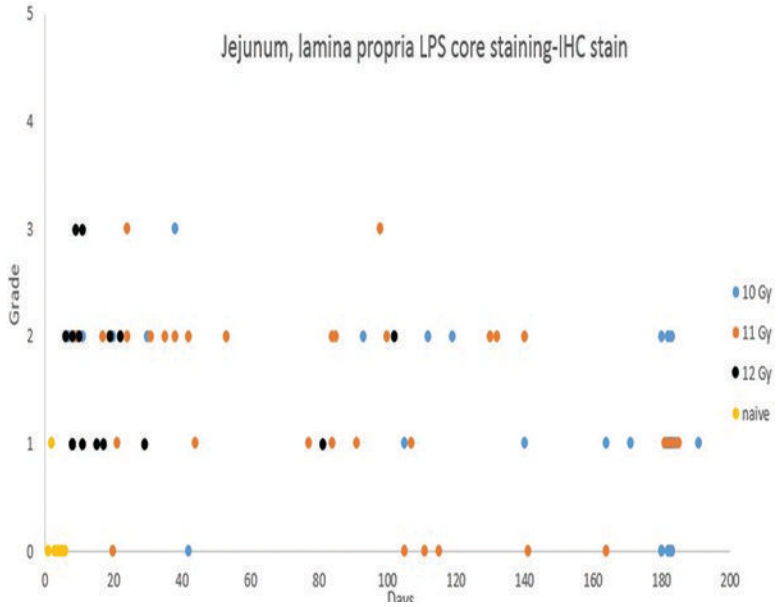

Figure 5a.

Immunohistochemical (IHC) staining for lipopolysaccharide (LPS) core in the lamina propria of the jejunum was not observed in 5 of 6 naïve control animals, and was grade 1 in the remaining naïve control animal. By contrast, LPS core staining, ranging from grade 1 to grade 3, was present in the lamina propria of the jejunal mucosa of 69 of the 82 irradiated animals in which an LPS IHC-stained section was available.

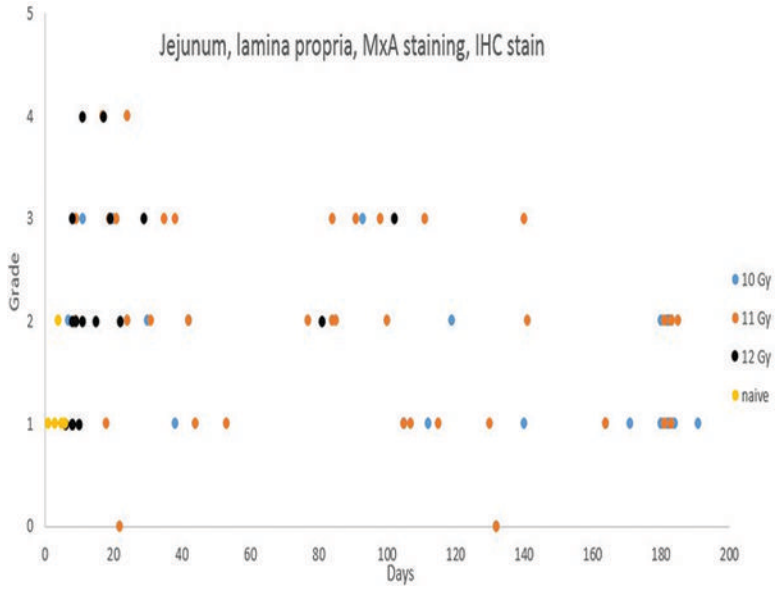

Figure 5b.

Immunohistochemical staining for MxA, indicating active immunocytes, revealed an increased number of positively stained immunocytes in the jejunal lamina propria of irradiated animals as compared to the predominantly grade 1 MxA-positive cellular population in the naïve control animals.

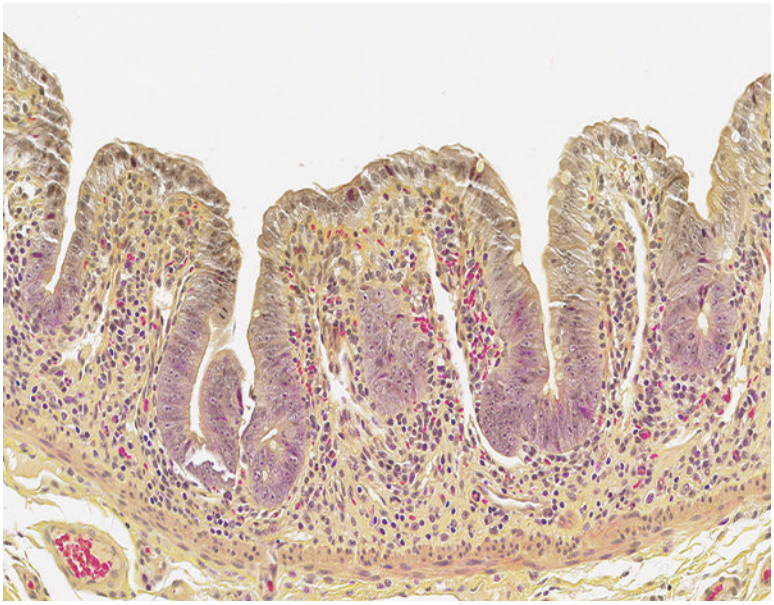

Figure 5c.

The jejunum of a male rhesus macaque collected at day 10 following irradiation at 12 Gy has severely blunted villi with proliferative crypt cells extending up the villi to the superficial mucosal surface. Note the absence of Paneth cells, as demonstrated in the following image. Erythrocytes within blood vessels and scattered in the lamina propria are stained a bright magenta color. Lendrum stain, 20x objective magnification.

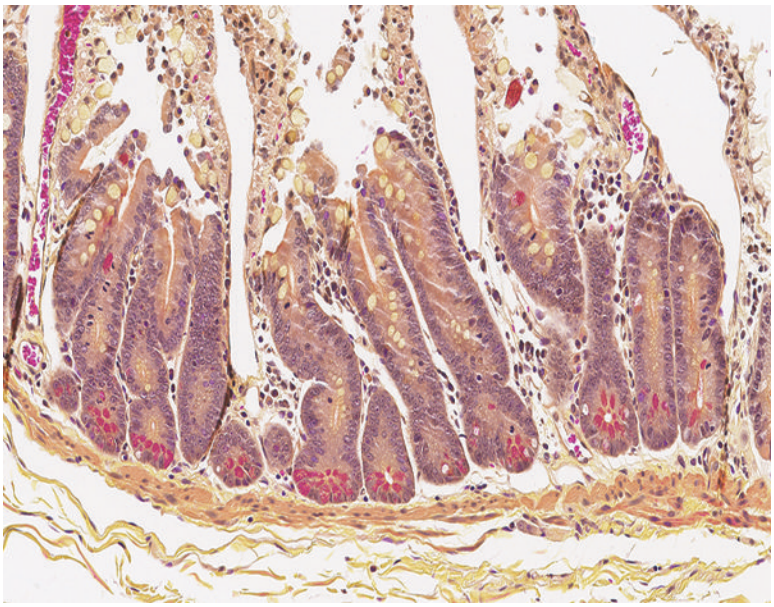

Figure 5d.

The jejunum of a male rhesus macaque collected at day 105 following irradiation at 10 Gy has numerous crypt Paneth cells containing brightly stained cytoplasmic granules, indicating recovery of the Paneth cell population. Lendrum stain, 20x objective magnification.

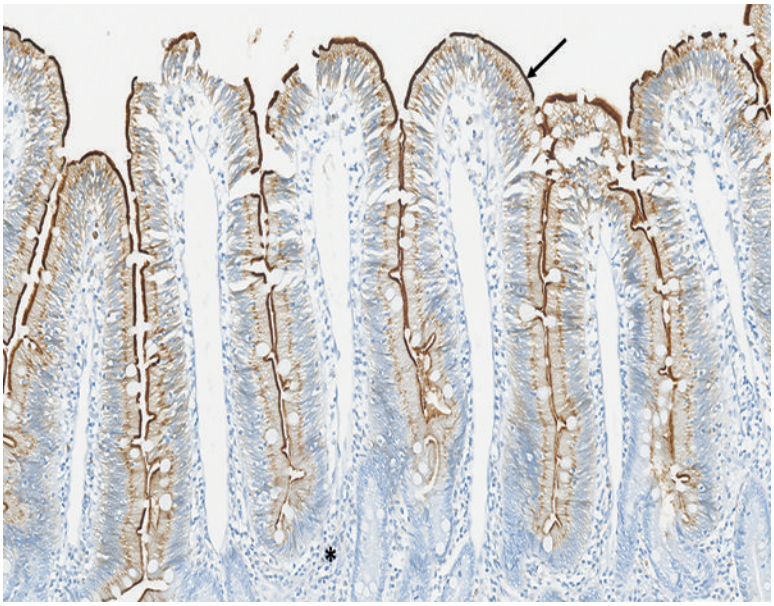

Figure 6a.

The jejunum of a naïve male rhesus macaque has prominent CD13-positive staining (arrow) of the brush border on the apical surface of intestinal epithelial cells. Note the absence of CD13-positive staining in the leukocytic population in the lamina propria (*). CD13 IHC stain, 15x objective magnification.

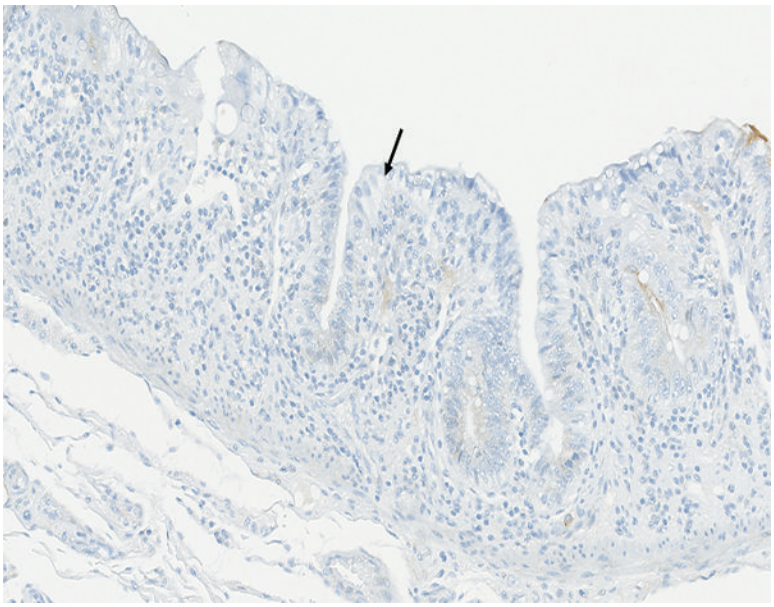

Figure 6b.

The jejunum of a male rhesus macaque collected at day 10 following irradiation at 12 Gy has no CD13-positive brush border on the surface of epithelial cells (arrow). CD13 IHC stain, 20x objective magnification.

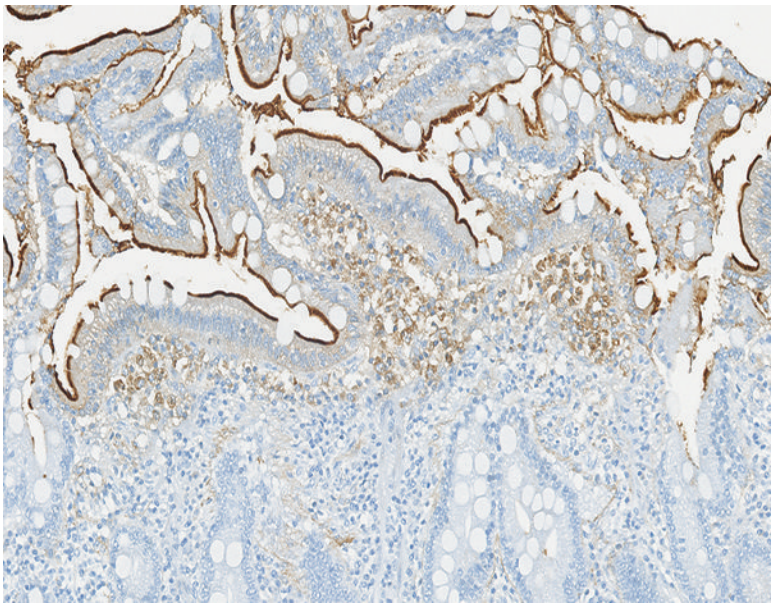

Figure 6c.

The jejunum of a male rhesus macaque collected at day 182 following irradiation at 10 Gy has intact CD13-positive brush border on the surface of epithelial cells (arrow) as well as a population of CD13-positive large mononuclear cells (*) in the superficial aspect of the mucosal lamina propria. CD13 IHC stain, 20x objective magnification.

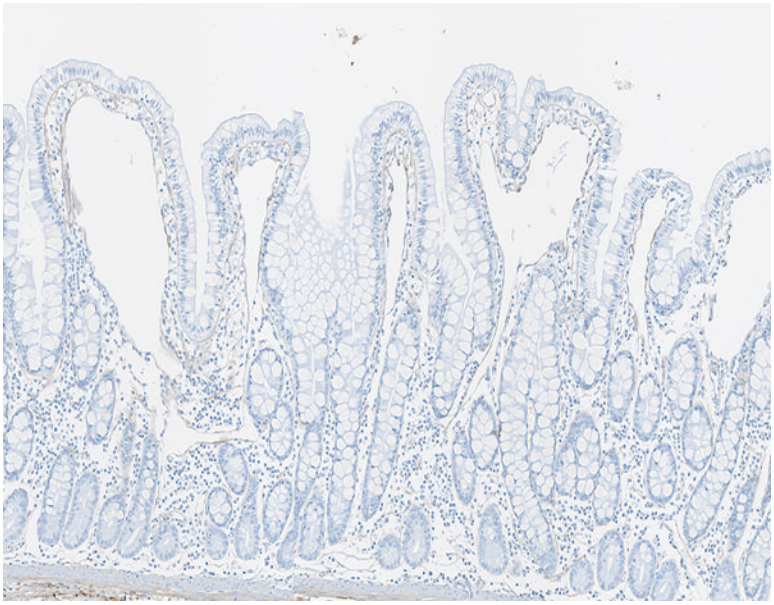

Figure 6d.

The jejunal mucosa of a naïve male rhesus macaque has a minimal number of fine, brown-stained collagen fibrils located primarily in the tips of villi. Collagen 1 IHC stain, 10x objective magnification.

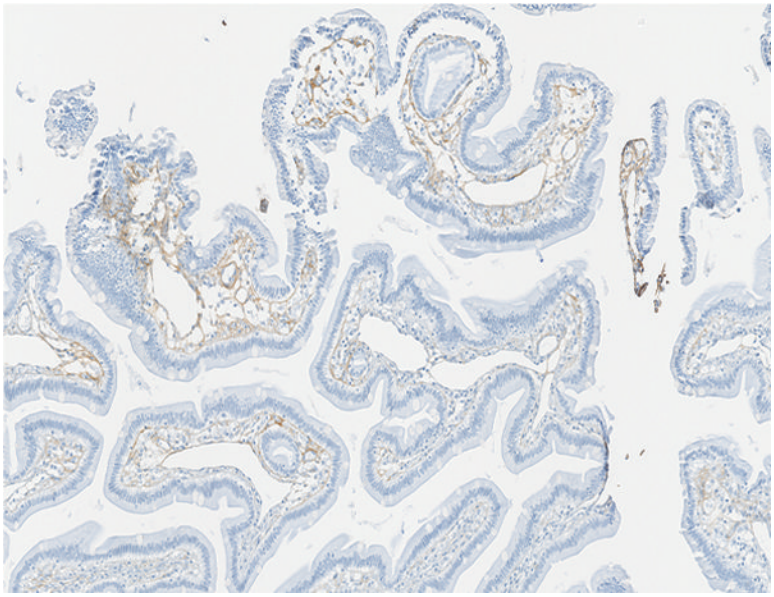

Figure 6e.

The jejunum of a male rhesus macaque collected at day 100 following irradiation at 11 Gy has more prominent collagen fibrils than were noted in the naïve control animals. Collagen 1 IHC stain, 10x objective magnification.

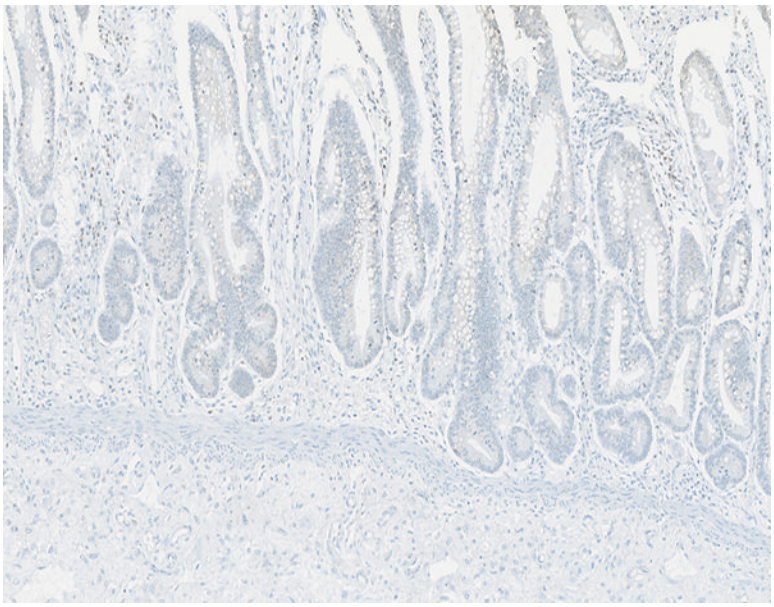

Figure 7a.

The jejunum of a male rhesus macaque collected at day 20 following irradiation at 10 Gy has no discernible connective tissue growth factor (CTGF) expression in crypt cells. CTGF IHC stain, 10x objective magnification.

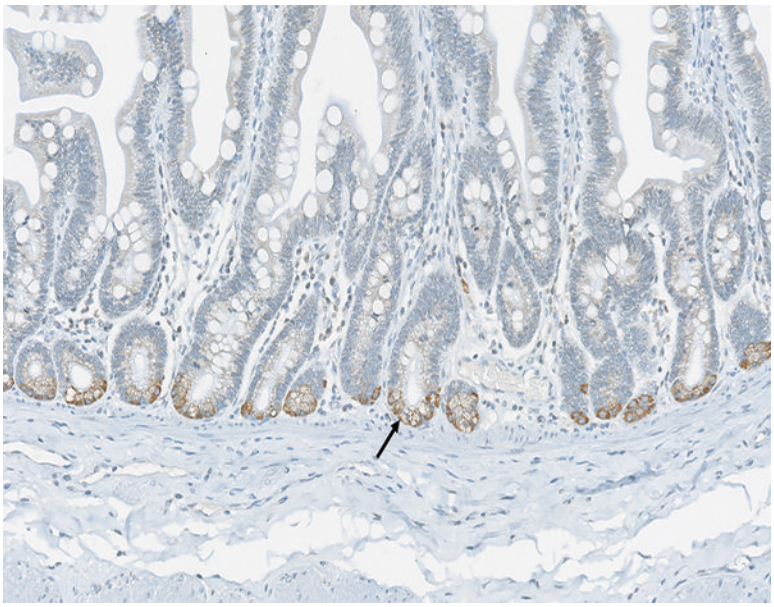

Figure 7b.

The jejunum of a male rhesus macaque collected at day 98 following irradiation at 11 Gy has numerous $CTGF^{+}$ cells (arrow) located in the bottom of crypts. CTGF IHC stain, 20x objective magnification.

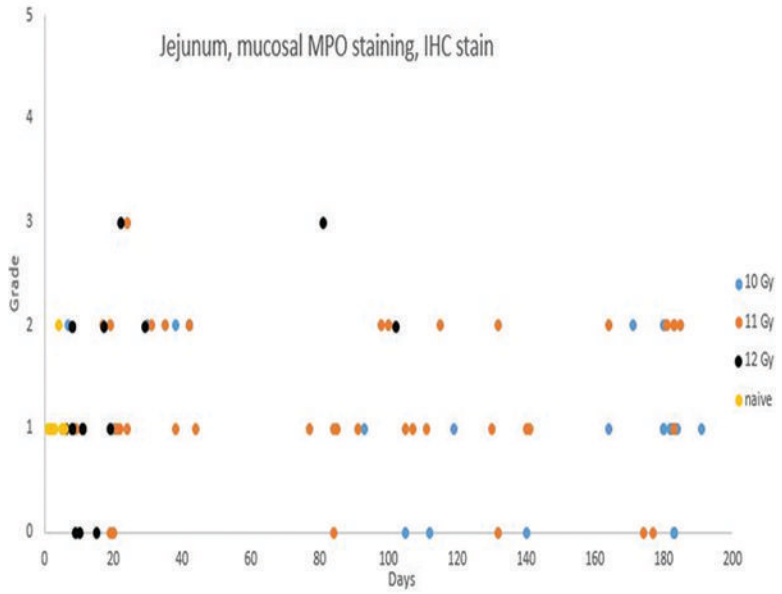

Figure 7c.

Immunohistochemical staining for myeloperoxidase revealed inflammatory cells such as neutrophils and macrophages. There was an indication of an increased population of these inflammatory cells in the jejunal mucosa of irradiated animals, but pronounced inflammatory reactions were not a major feature of the radiation injury to the jejunum.

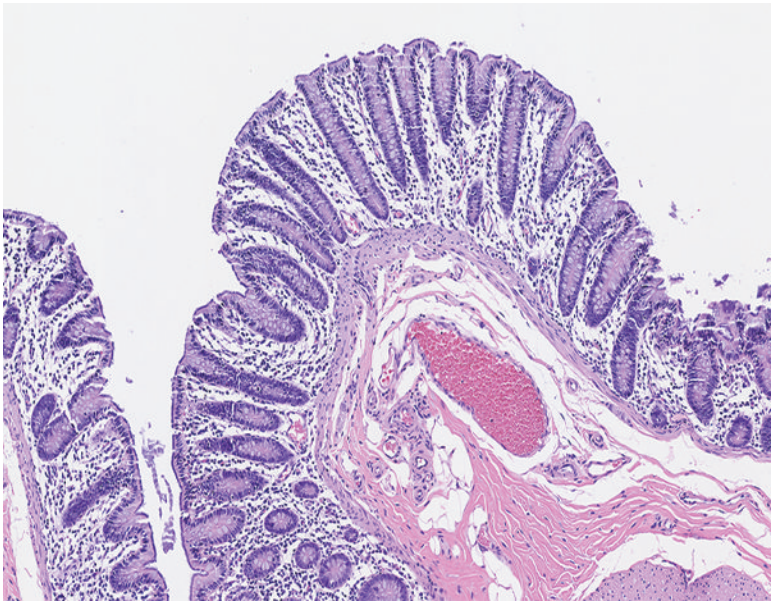

Figure 8a.

The colon of a naïve control rhesus macaque has an orderly array of colonic crypts and a thin superficial layer of mature epithelial cells. The folded contour of the colonic mucosa is evident in this image. H&E stain, 10x objective magnification.

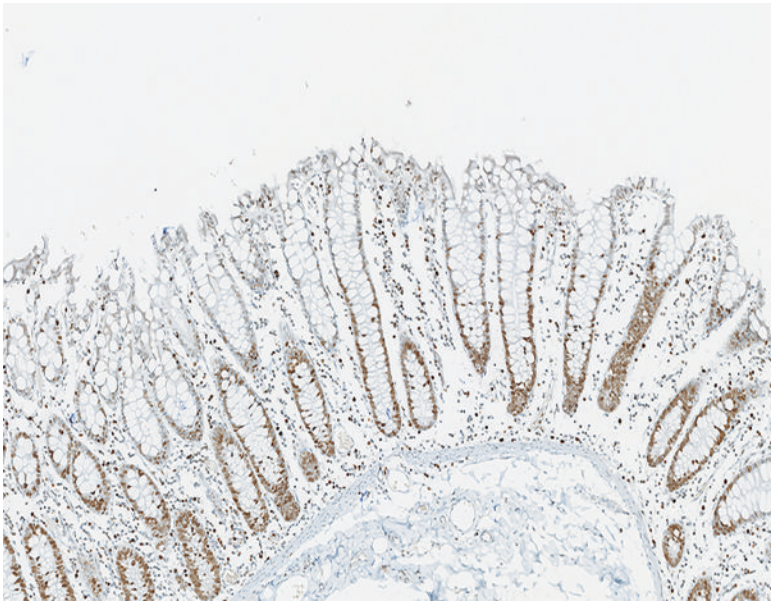

Figure 8b.
The colon of a naïve control rhesus macaque has extensive crypt cell proliferation as revealed by the brown chromagen deposition in cellular nuclei. Ki67 IHC stain, 10x objective magnification.

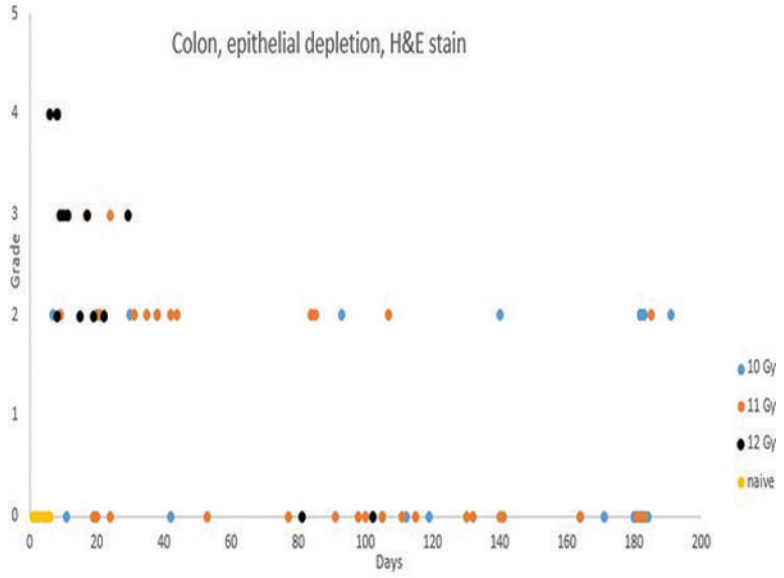

Figure 8c.

Post-irradiation epithelial depletion in the colon was most commonly observed in animals that were necropsied in the first 40 days post-irradiation, but was present to some extent in animals necropsied throughout the period of observation.

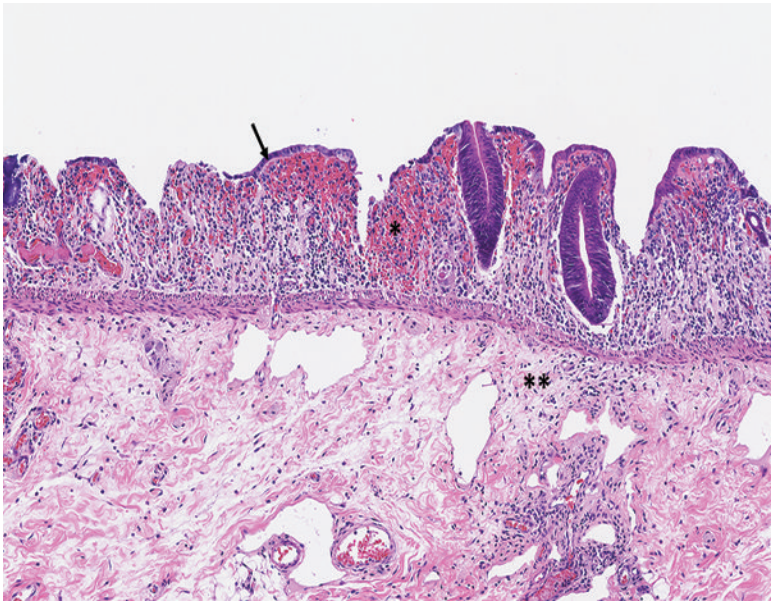

Figure 8d.

The colon of a male rhesus macaque collected at day 8 following irradiation at 12 Gy has severe epithelial depletion with mucosal hemorrhage (*), submucosal edema (**), densely basophilic regenerative crypts, and sparsely populated areas of superficial regenerative epithelial cells (arrow). H&E stain, 10x objective magnification.

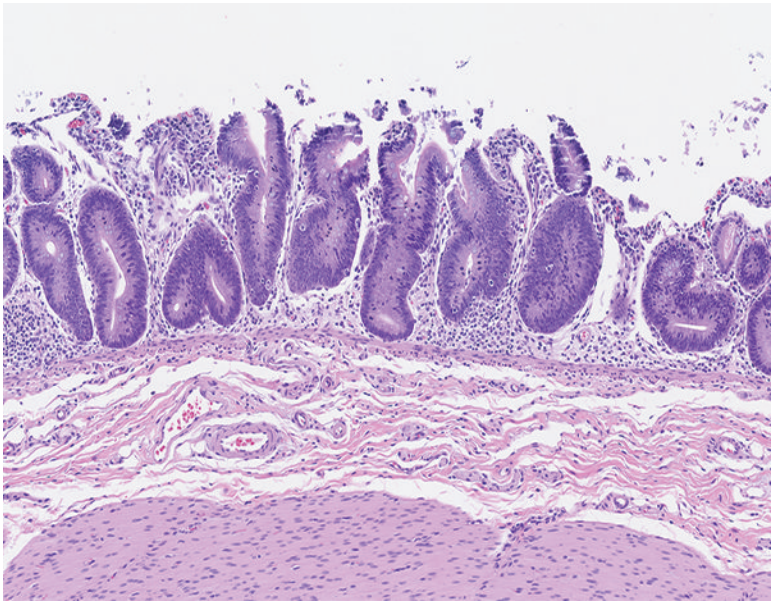

Figure 8e.

The colon of a male rhesus macaque collected at day 17 following irradiation at 11 Gy has pronounced proliferative activity in crypts, with little remaining of the overlying normal epithelium. H&E stain, 10x objective magnification.

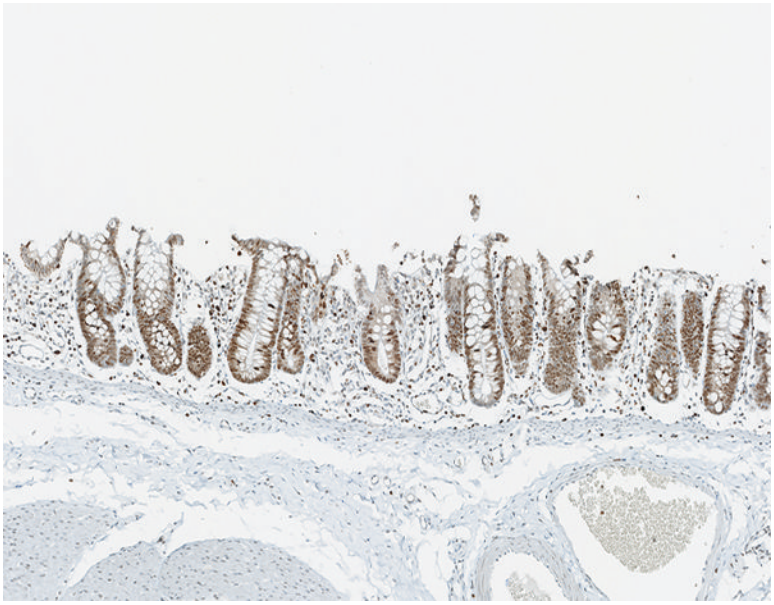

Figure 8f.

The colon of a male rhesus macaque collected at day 17 following irradiation at 11 Gy has extensive proliferative activity in crypts (*). Note the superficial zone of normal, nonproliferative epithelial cells that are visible in the colon of the naïve control animal (above) is not present in this image. Ki67 IHC stain, 10x objective magnification.

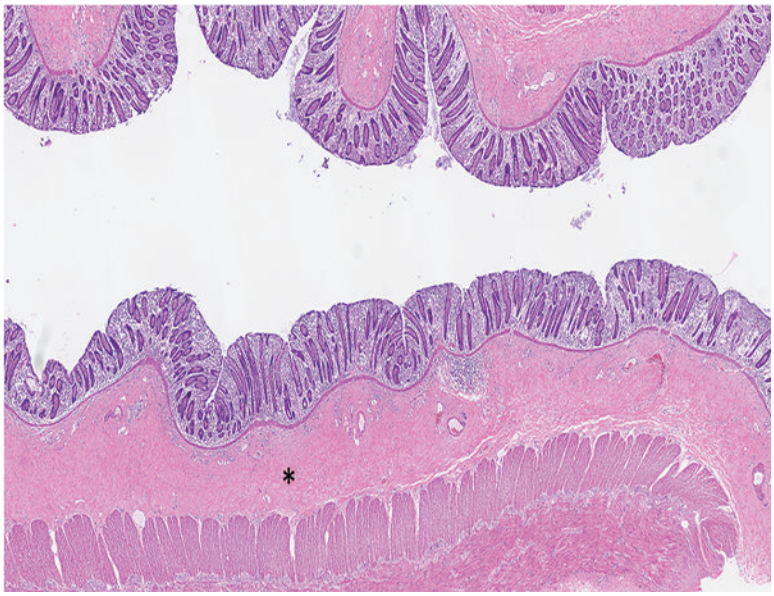

Figure 9a.

Colon of a male rhesus macaque collected at day 102 following irradiation at 12 Gy has dense fibrous connective tissue in the submucosa (*). H&E stain, 2.5x objective magnification.

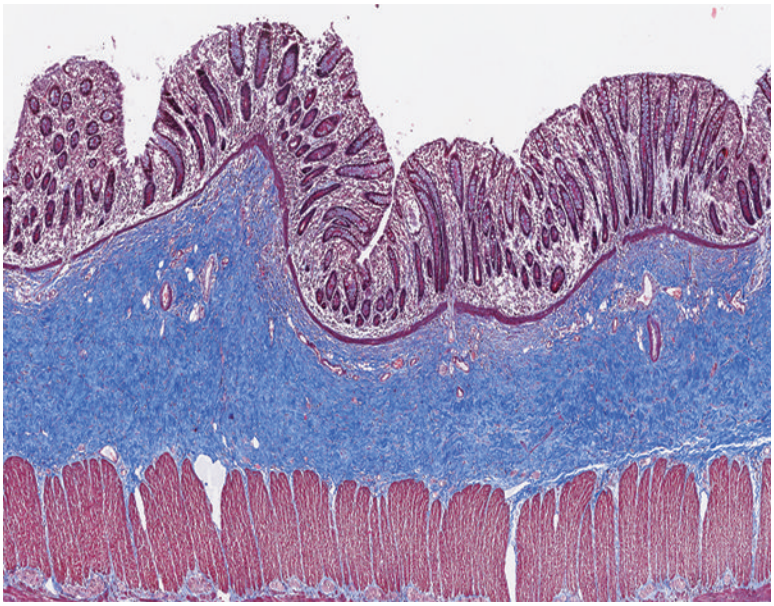

Figure 9b.
The colon of a male rhesus macaque collected at day 102 following irradiation at 12 Gy has dense blue-stained collagen in the submucosa. Masson's trichrome stain 5x objective magnification.

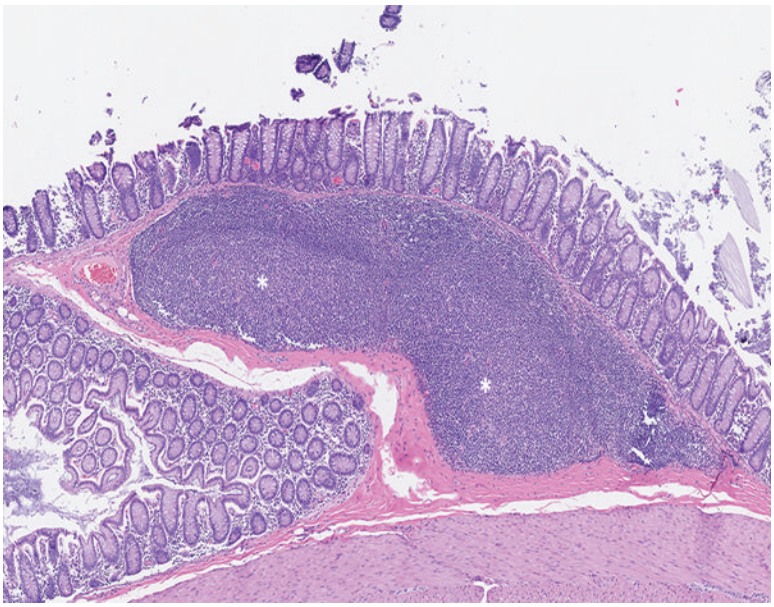

Figure 9c.

The colonic lymphoid follicle (lymphoglandular complex) of a naïve control rhesus macaque is highly cellular, with prominent germinal centers (*) located at the base of the follicular structure. Note the thick layer of colonic mucosa overlying the lymphoid follicle. H&E stain, 5x objective magnification.

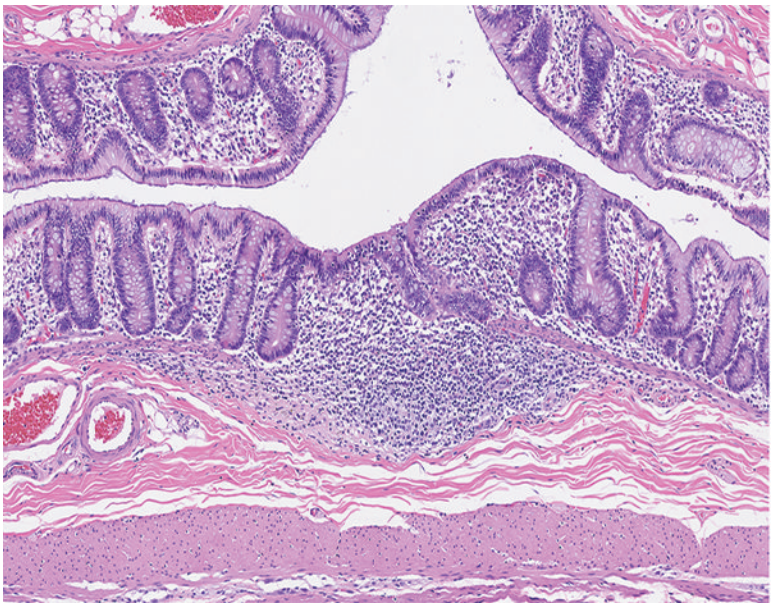

Figure 9d.

The colonic lymphoid follicle (lymphoglandular complex) of a rhesus macaque at day 37 following irradiation at 11 Gy has markedly reduced cellularity, with no discernible germinal centers. Corticosteroid administration as part of medical management had not commenced at this time in the study, thus the observed changes were unequivocally radiation-related. H&E stain, 10x objective magnification.

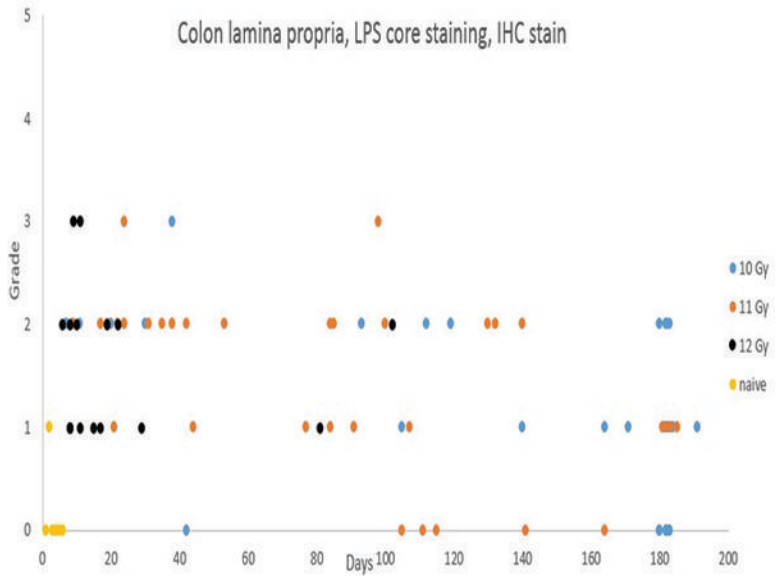

Figure 9e.

Immunohistochemical staining for lipopolysaccharide (LPS) core revealed an increased population of LPS core-positive cells in the colonic mucosa of irradiated animals necropsied throughout the observation period. Compare this staining pattern to the MxA (Figure 12d) staining in the medullary region of the mesenteric lymph node.

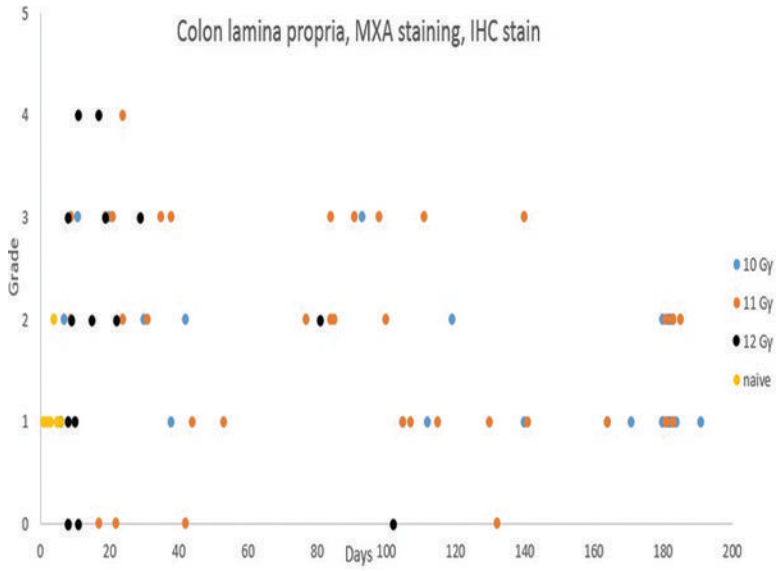

Figure 9f.

Immunohistochemical staining for MXA, indicating active immunocytes, revealed a variable degree of positive staining in the colonic lamina propria throughout the observation period. The lamina propria MXA staining was more pronounced in animals irradiated at 11 and 12 Gy, presumably reflecting a greater level of mucosal injury and associated inflammation with the higher radiation doses.

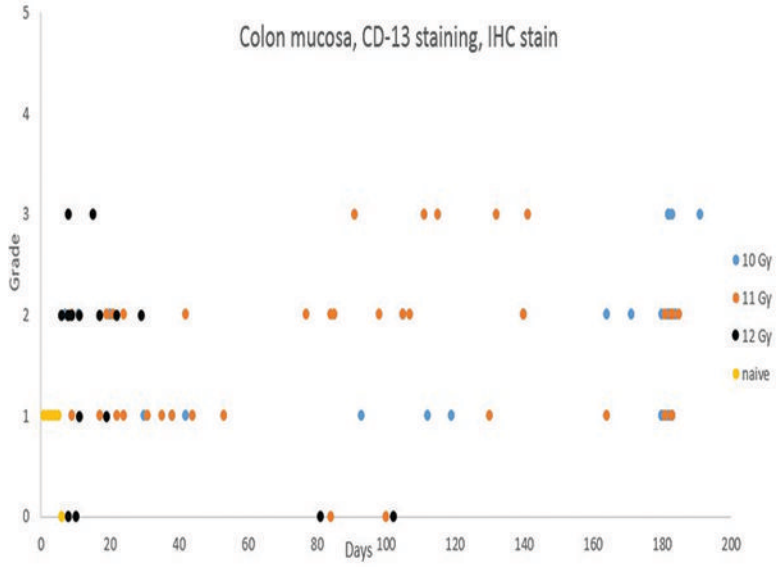

Figure 10a.
CD13 staining of colonic mucosal leukocyte populations was increased in irradiated animals.

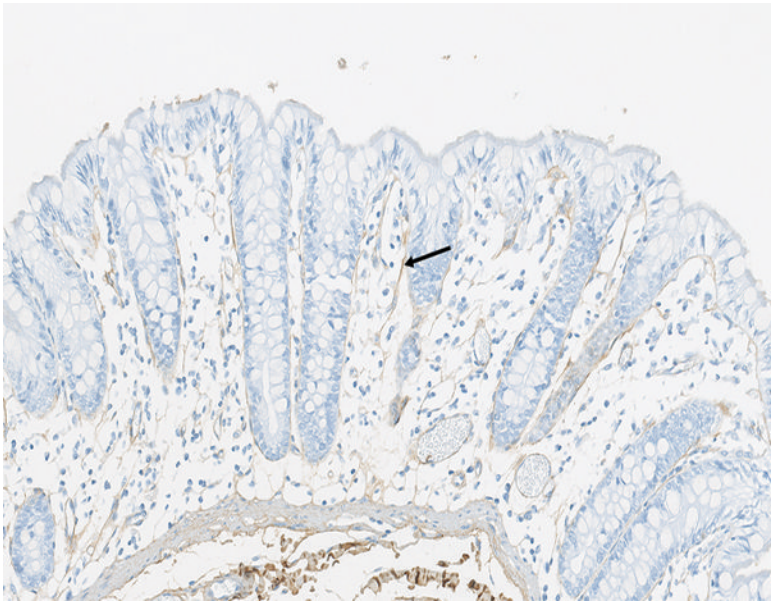

Figure 10b.
The colon of a naïve male rhesus macaque has fine collagen fibrils (arrow) located in the mucosal lamina propria. Collagen 1 IHC stain, 20x objective magnification.

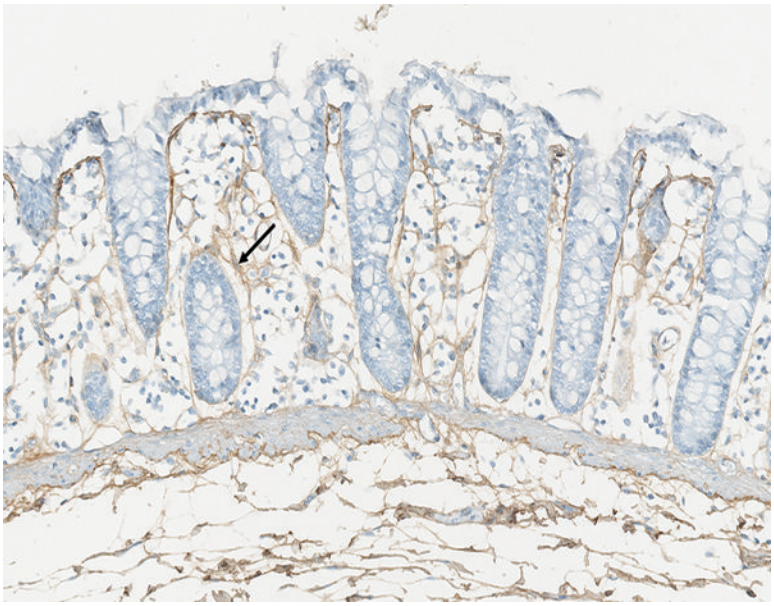

Figure 10c.
The colon of a male rhesus macaque collected at day 183 following irradiation at 10 Gy has an increased amount of fibrillar collagen (arrow) in the mucosal lamina propria. Collagen 1 IHC stain, 20x objective magnification.

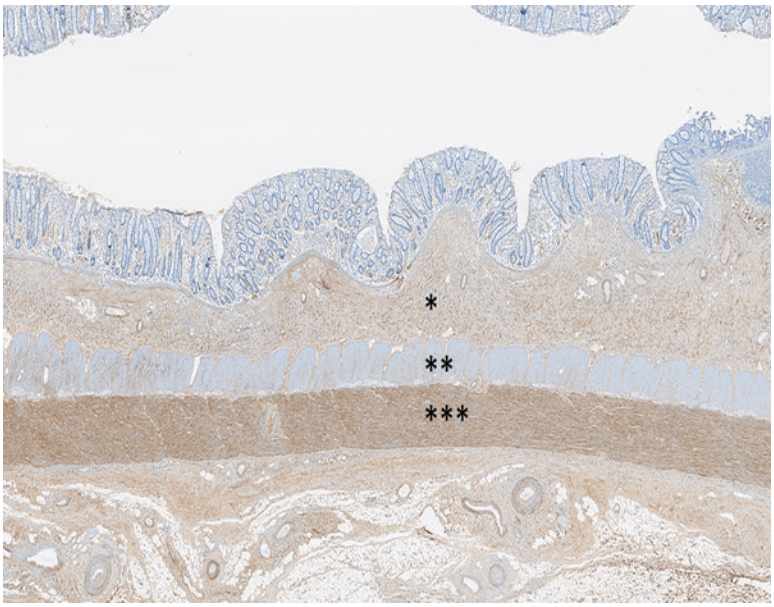

Figure 10d.

The colon of a male rhesus macaque collected at day 102 following irradiation at 12 Gy has a markedly increased amount of collagen in the submucosa (*) and external layer of the muscularis externa (***). Note the relative sparing of the internal layer of the muscularis externa (**). There is an increased amount of collagen in the mesocolic attachment at the bottom of the image. Collagen 1 IHC stain, 20x objective magnification.

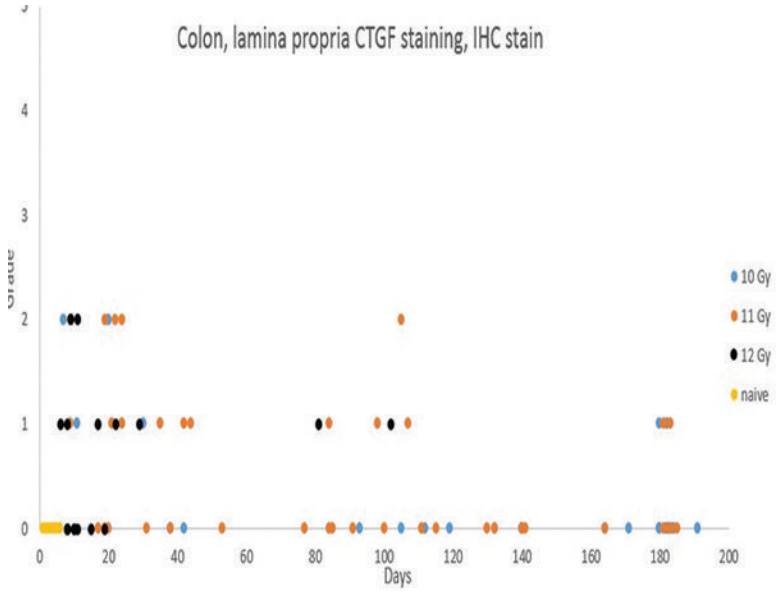

Figure 10e.

Immunohistochemical staining for connective tissue growth factor (CTGF) revealed positive staining in leukocyte/macrophage populations in the lamina propria of the colonic mucosa of irradiated animals. The increased $CTGF^{+}$ cell population in the colon was most commonly noted in animals necropsied within 50 days of irradiation.

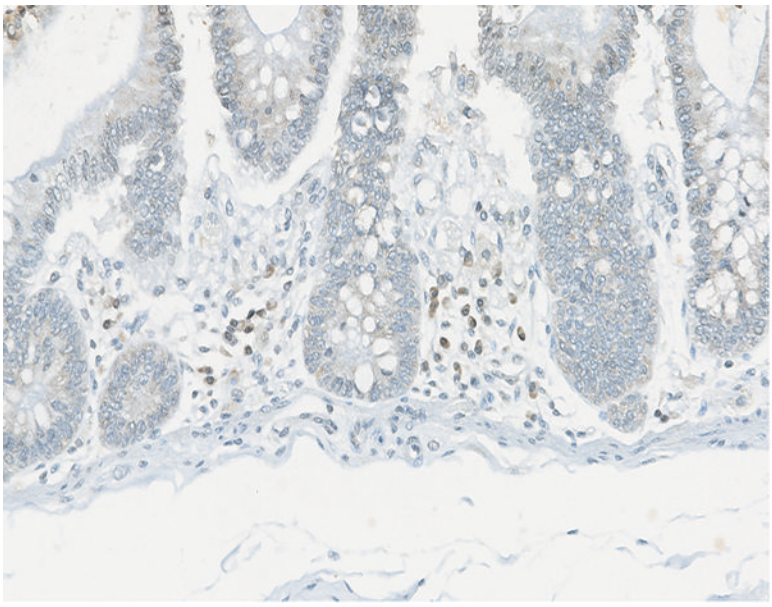

Figure 10f.

The colonic mucosal lamina propria (*) of a male rhesus macaque collected at day 20 following irradiation at 10 Gy has individualized cells that exhibit low-intensity connective tissue growth factor (CTGF) staining. CTGF IHC stain, 30x objective magnification.

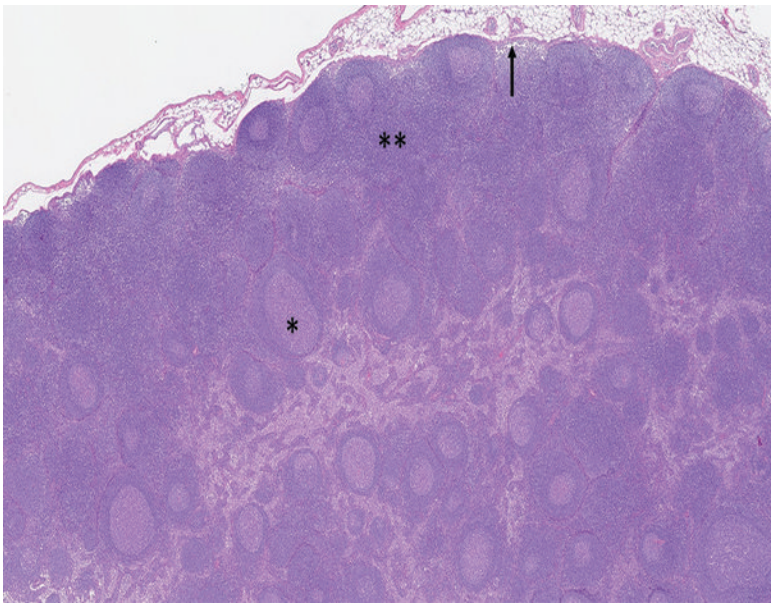

Figure 11a.

The histologic section of mesenteric lymph node from a naïve adult male rhesus macaque has highly cellular cortex (**) and prominent germinal centers (*). Subcapsular sinuses (arrow) receive lymph and cellular elements from tissues drained by the lymph node. H&E stain, 2.5x objective magnification.

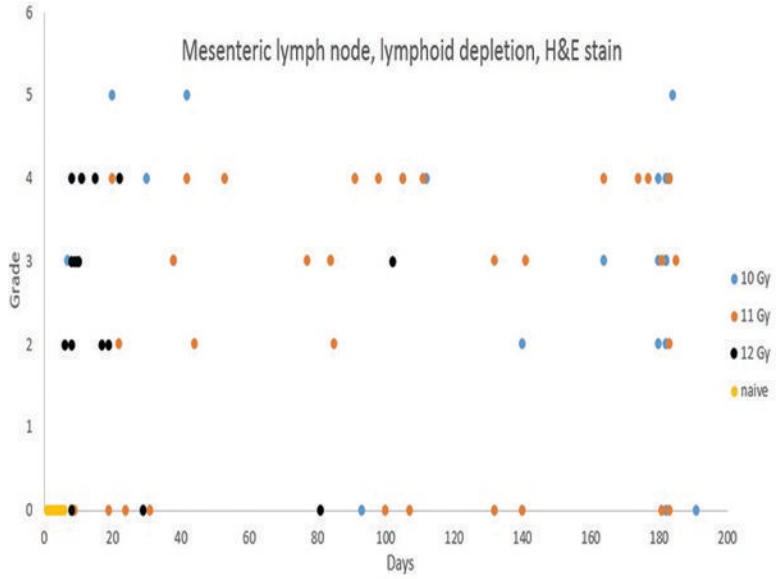

Figure 11b.

Depletion of lymphoid elements in lymph nodes is a well-known effect of irradiation, and was amply demonstrated in the present study. Lymphoid depletion before post-irradiation day 42 was unequivocally associated with irradiation, but thereafter the interpretation of lymphoid depletion was complicated by the administration of corticosteroids used in medical management.

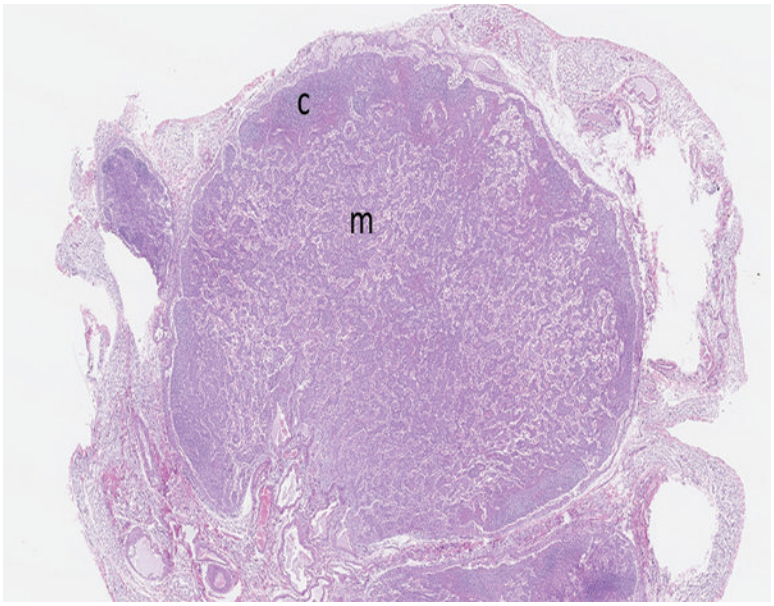

Figure 11c.

The mesenteric lymph node of a male rhesus macaque collected at day 11 following irradiation at 12 Gy has reduced cortical (c) cellularity and a uniform pattern of cords and sinuses remaining in the medulla (m). H&E stain, 1.75x objective magnification.

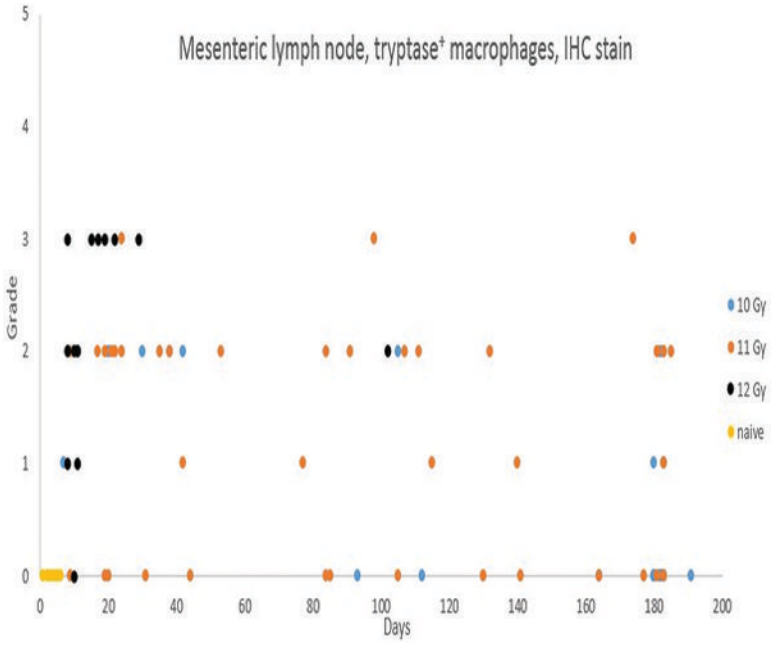

Figure 11d.

In contrast to the tryptase staining results for mast cells, there was a distinct radiation-associated increase in the population of tryptase-positive macrophages in subcortical sinuses of irradiated animals. This was most commonly noted in animals necropsied during the first 50 days following irradiation, and was more common and more pronounced in animals irradiated at 12 Gy.

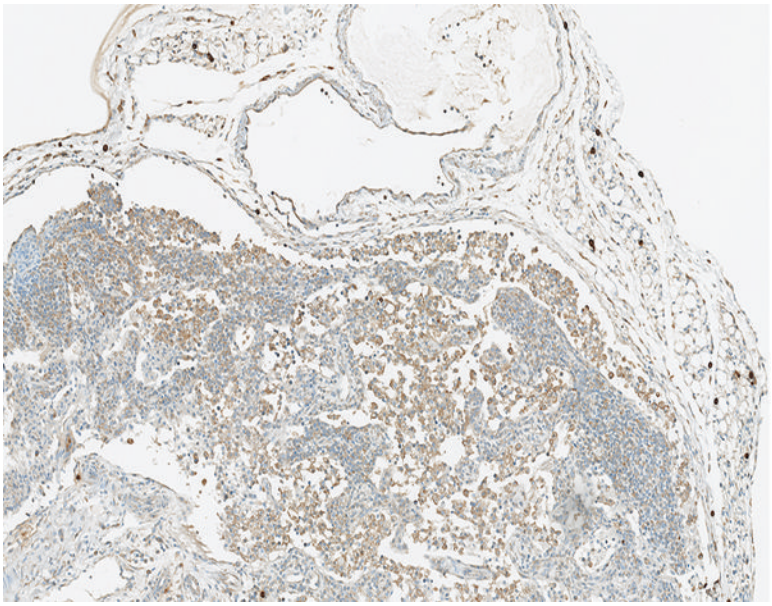

Figure 11e.

The mesenteric lymph node of a male rhesus macaque collected at day 17 following irradiation at 12 Gy has reduced cortical cellularity and numerous tryptase^{+} histiocytic cells within subcapsular sinuses and cortical sinuses. Tryptase IHC stain, 10x objective magnification.

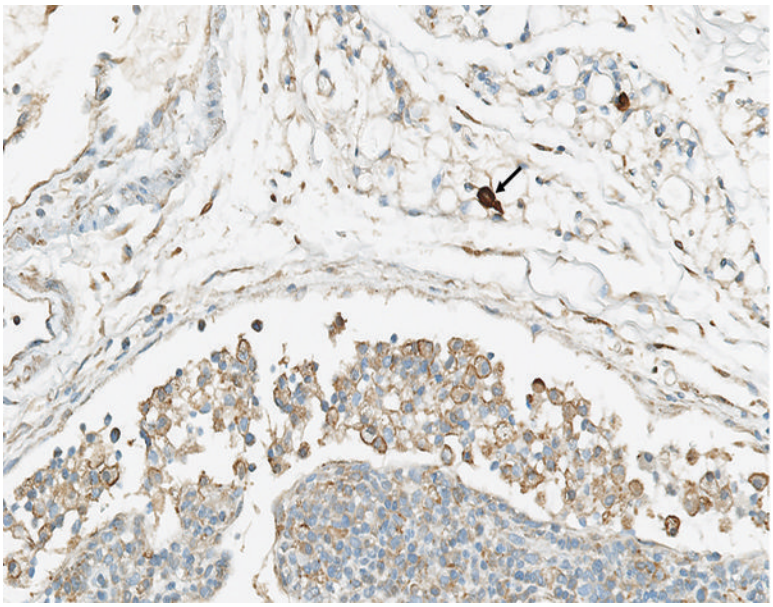

Figure 11f.

A higher magnification view of the previous image reveals the tryptase staining is localized on the surface of histiocytic cells, resulting in a thin brown line at the margin of the cells. Note the densely stained mast cells (arrow) in the areolar tissue near the lymph node. Tryptase IHC stain, 30.8x objective magnification.

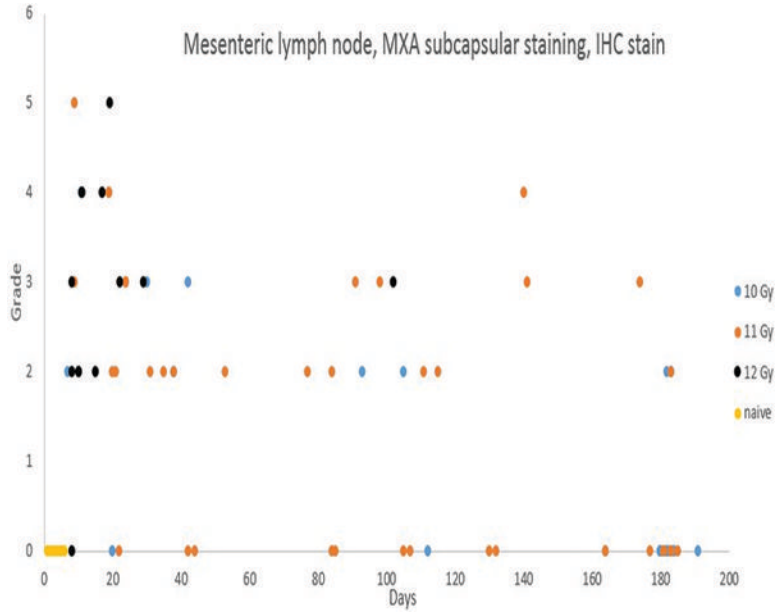

Figure 12a.

Immunohistochemical staining for MXA was commonly noted in cells located in the subcapsular sinuses of mesenteric lymph nodes of irradiated animals, but not in the naïve control animals. The stained cells were consistent with activated immunocytes that were migrating to the mesenteric lymph nodes from the intestinal tract. There was no discernible incidence pattern relative to radiation level or post-irradiation interval.

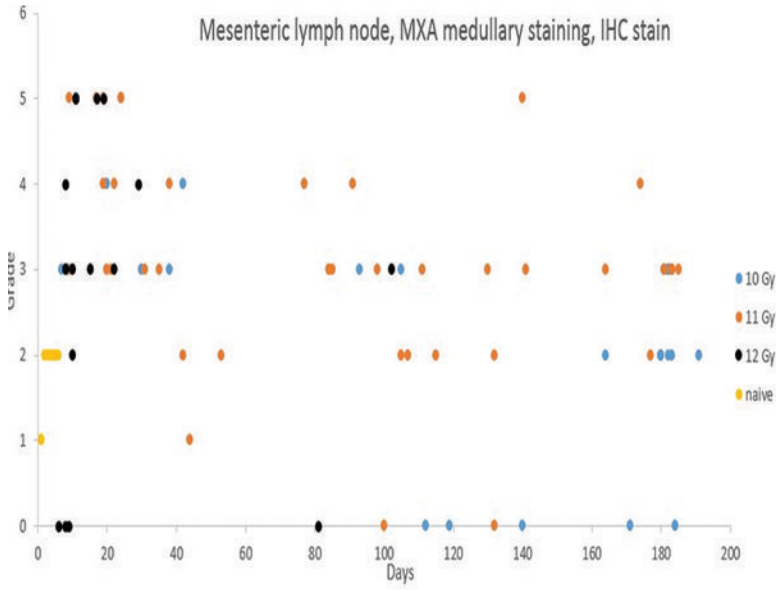

Figure 12b.

Cells staining positively for MXA were commonly noted in the medullary region of mesenteric lymph nodes, including the naïve control animals, but a greater number of MxA-positive cells was present in the irradiated animals versus the naïve control animals.

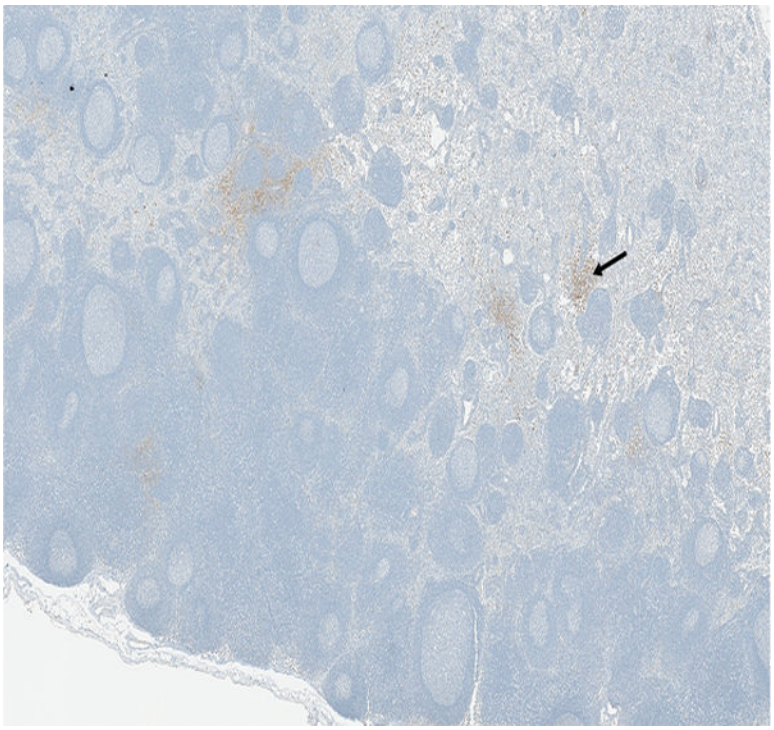

Figure 12c.

The histologic section of mesenteric lymph node from a naive adult male rhesus macaque has multiple aggregations of positively stained cells (arrow), indicating clusters of activated immunocytes. MxA IHC stain, 2.5x objective magnification.

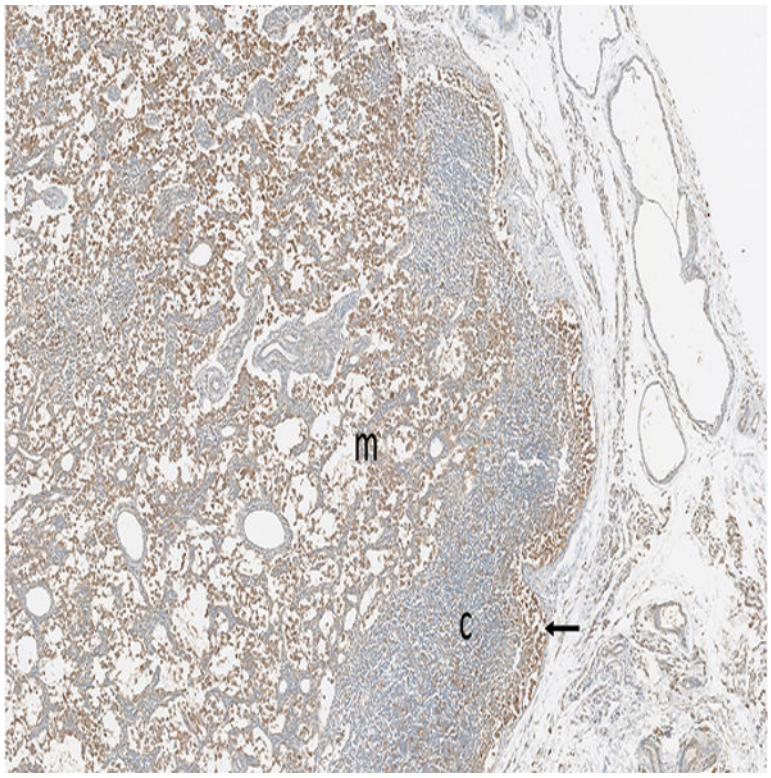

Figure 12d.

The mesenteric lymph node of a male rhesus macaque collected at day 22 following irradiation at 11 Gy has a large number of MxA^{+} (activated) immunocytes in the medulla (m), with a smaller number in the hypocellular cortex (c). Note the accumulation of activated immunocytes in the subcapsular sinus (arrow), indicating activated cells are arriving from peripheral tissues. MxA IHC stain, 5x objective magnification.

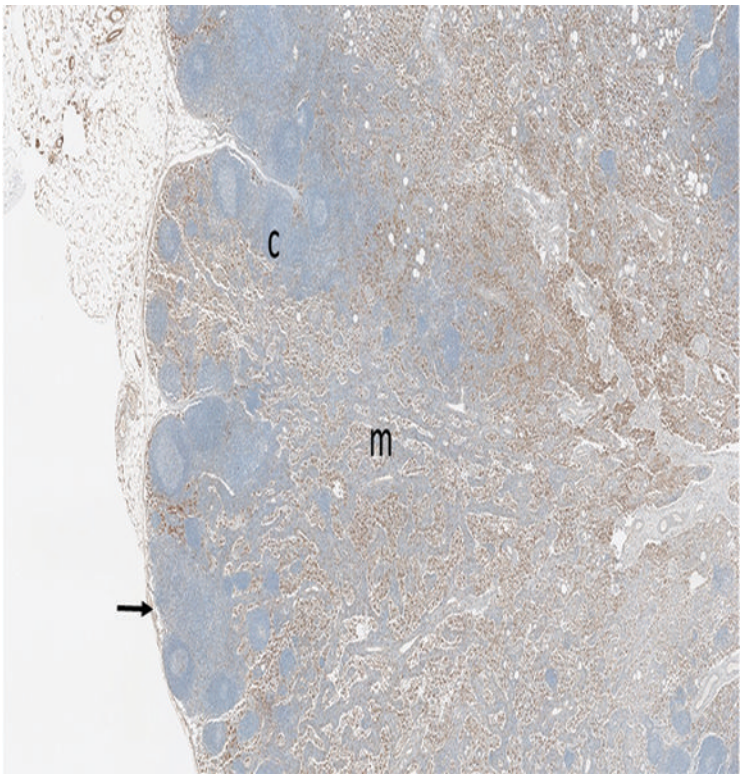

Figure 12e.

The mesenteric lymph node of a male rhesus macaque collected at day 183 following irradiation at 10 Gy has numerous MxA^{+} (activated) immunocytes in the medulla (m), but fewer in the cortex (c) and subcapsular sinuses (arrow). Presence of activated immunocytes in the medullary region suggests an immunological response is ongoing 183 days after irradiation, but the relative sparse population of MxA+ cells in the subcapsular sinuses suggests diminution in the population of activated immunocytes that are migrating into the lymph node from the intestine. The jejunum of this animal had grade 3 MxA staining in the lamina propria, grade 2 LPS core staining in the lamina propria, and grade 3 connective tissue growth factor staining in crypts, but the examined jejunal specimens had no histologic evidence of an active inflammatory reaction. MxA IHC stain, 2.5x objective magnification.

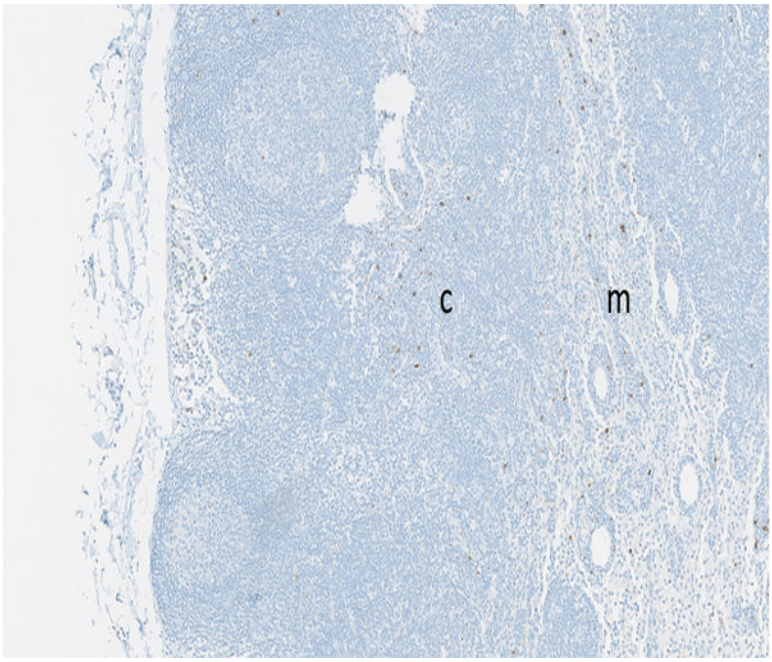

Figure 13a.

The mesenteric lymph node from a naive adult male rhesus macaque has widely scattered brown-stained myeloperoxidase-positive cells in the cortex (c) and medulla (m), reflecting the normal population of macrophages and neutrophils that exist within lymph nodes. MPO IHC stain, 10x objective magnification.

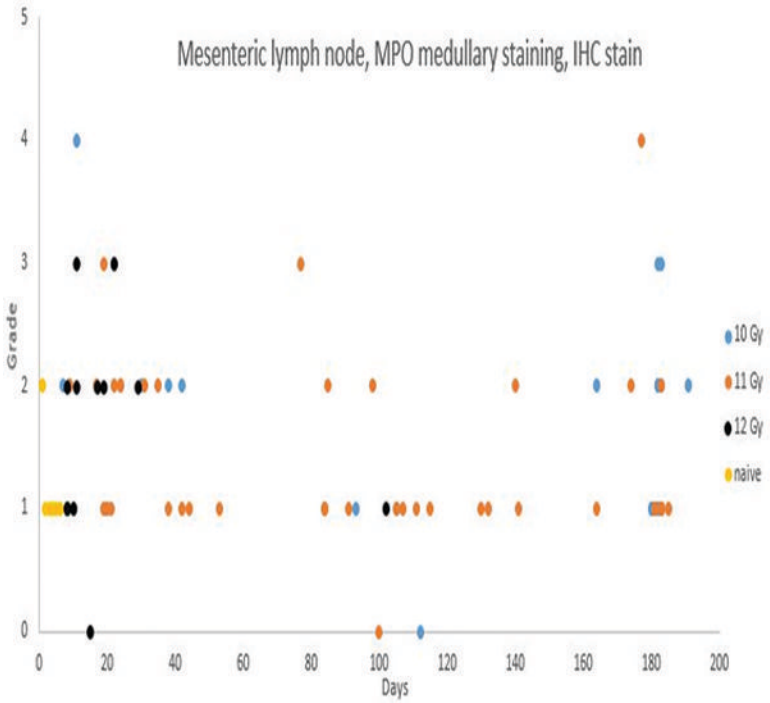

Figure 13b.

Immunohistochemical staining for myeloperoxidase (MPO) revealed MPO-positive cells in the medullary region of mesenteric lymph nodes of animals irradiated at 10, 11 or 12 Gy. The increased MPO-positive cell populations were most commonly seen in animals necropsied within 45 days of irradiation, with less common involvement of animals necropsied through the remainder of the observation period. The MPO-positive cells in medullary regions were microscopically consistent with macrophage/histiocyte populations.

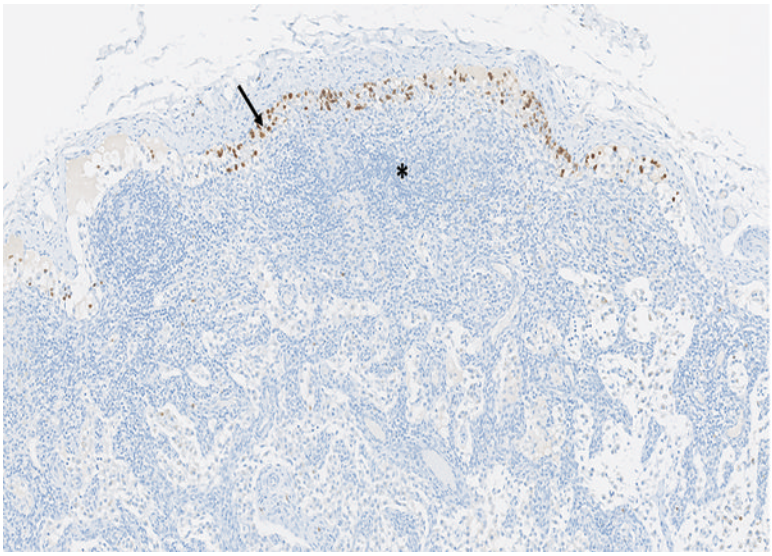

Figure 13c.

The mesenteric lymph node of a male rhesus macaque collected at day 8 following irradiation at 12 Gy has numerous myeloperoxidase (MPO)-positive cells within subcapsular sinuses (arrow), indicating migration of MPO-positive cells from the intestine. Note the sparse cellularity of the cortex (*) resulting from radiation-associated depletion of lymphoid cellular elements. MPO IHC stain, 10x objective magnification.

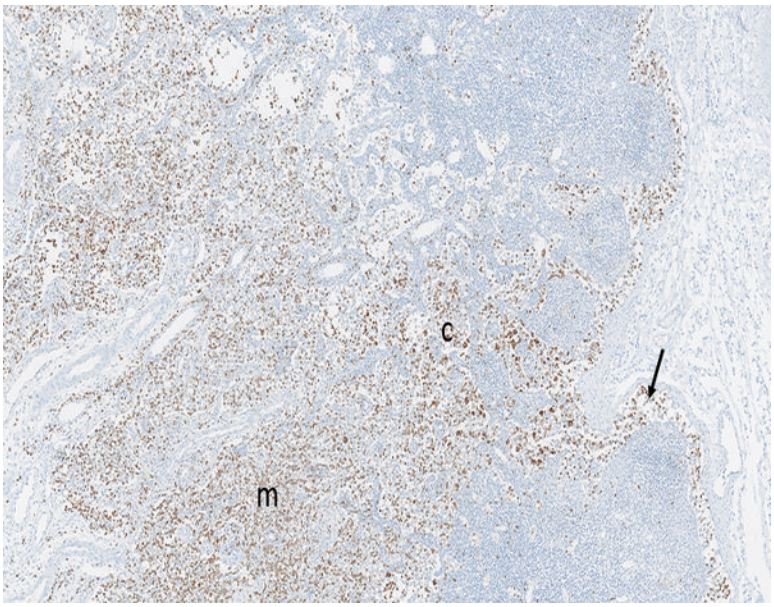

Figure 13d.
The mesenteric lymph node of a male rhesus macaque collected at day 11 following irradiation at 10 Gy has numerous myeloperoxidase-positive cells in subcapsular (arrow), cortical (c), and medullary (m) sinuses. MPO IHC stain, 2.5x objective magnification.

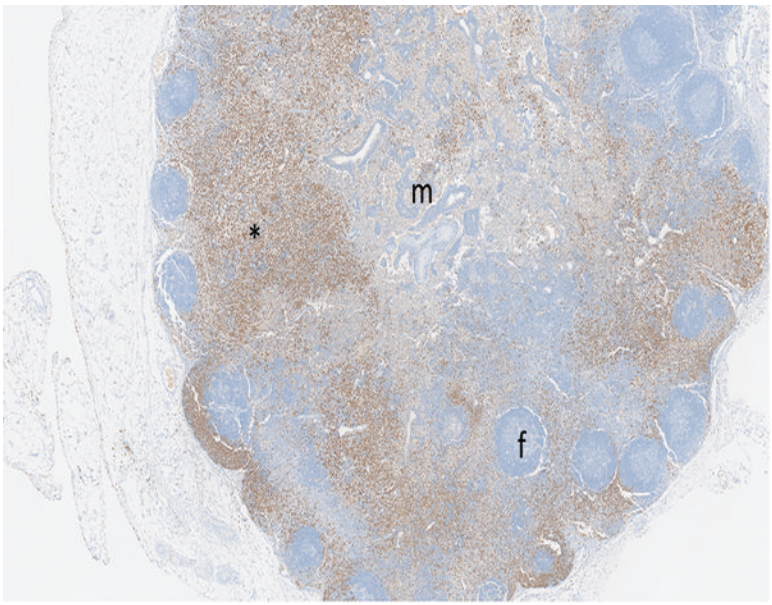

Figure 13e.

The mesenteric lymph node of a male rhesus macaque collected at day 177 following irradiation at 11 Gy has numerous myeloperoxidase-positive cells in the paracortex (*), with fewer stained cells in the medulla (m) and cortical follicles (f). The mesenteric lymph node of this animal had grade 4 bacterial invasion, grade 3 lymphoid depletion, grade 4 myeloperoxidase staining in subcapsular sinuses and medulla, grade 2 transforming growth factor-beta staining in subcapsular sinuses and medulla, and grade 2 connective tissue growth factor staining of cells in the medulla. The animal received a single dose of dexamethasone on post-irradiation day 177, the day the animal was euthanized. The jejunum and colon were not available for histological examination, but the lung was noted to have grade 4 bacterial invasion of the pleural surface, suggesting widespread septicemia. MPO IHC stain, 2.5x objective magnification.

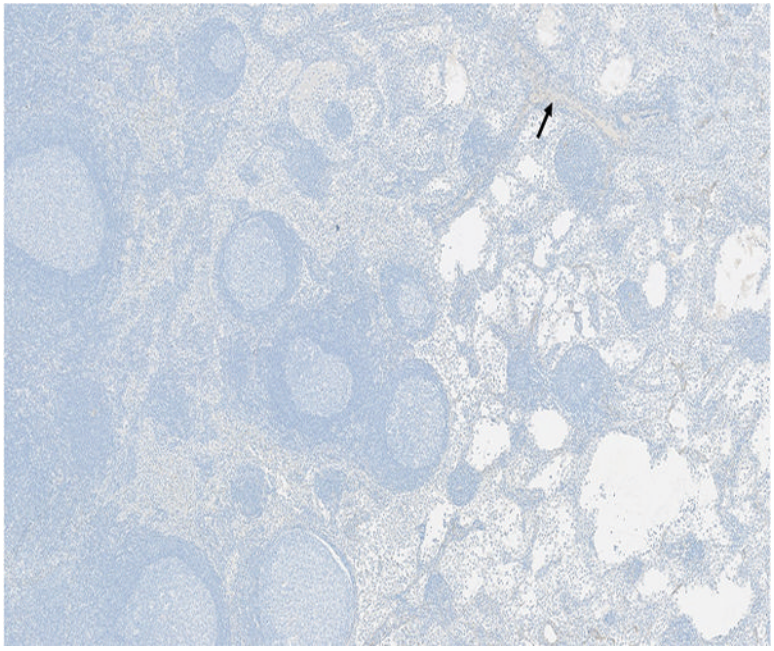

Figure 14a.

The histologic section of mesenteric lymph node from a naive male rhesus macaque has a small amount of faintly stained collagenous tissue (arrow) that is largely concentrated around vascular tracts in the medulla. Collagen 1 IHC stain, 5x objective magnification.

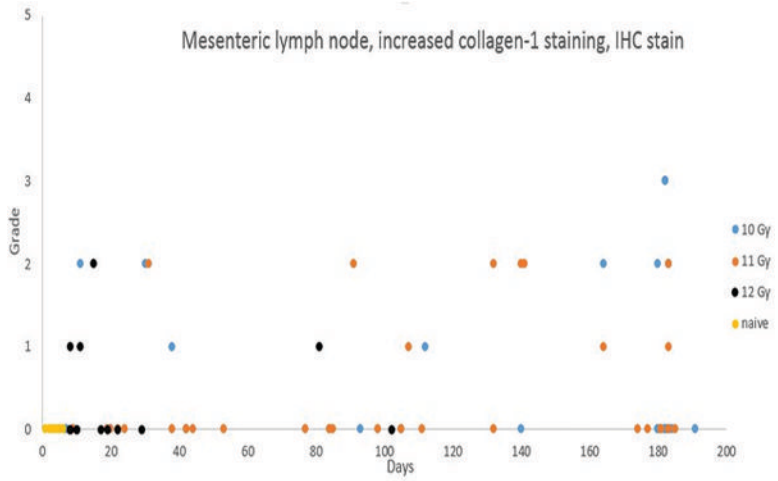

Figure 14b.

Immunohistochemical staining for collagen 1 revealed low-level increases in collagen deposition in lymph nodes of animals necropsied throughout the observation period, with no discernible distribution relative to radiation dose or post-irradiation interval. It should be noted that none of the animals irradiated at 12 Gy survived beyond post-irradiation day 102, therefore, any radiation dose-related influence on fibrosis incidence would not be detectable. Only two animals in the 12 Gy irradiation group survived beyond 30 days, and one of those animals had fibrosis of the mesenteric lymph nodes.

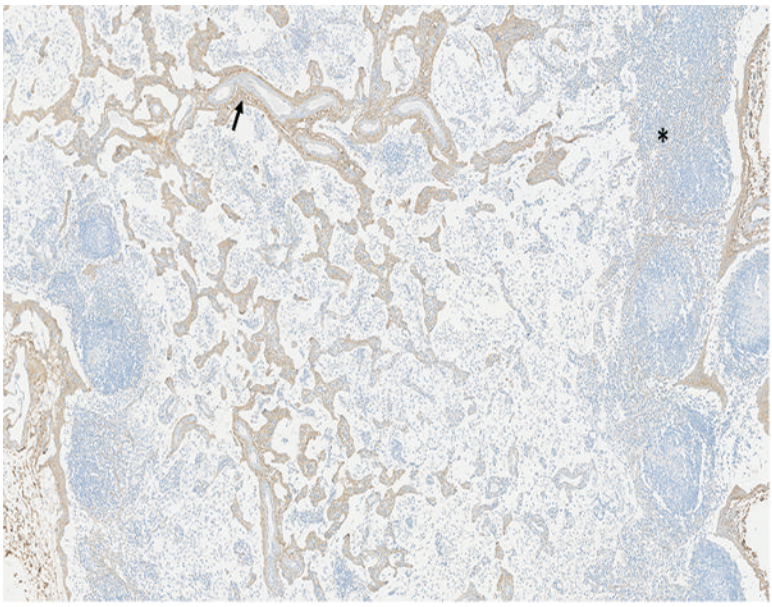

Figure 14c.

The mesenteric lymph node of a male rhesus macaque collected at day 130 following irradiation at 11 Gy has a pronounced increase in the amount of collagenous tissue (arrow) surrounding vascular tracts in the medulla. An increased amount of faintly stained collagenous tissue is discernible in the cortex (*). Densely stained collagenous tissue at the right margin of the image is the normal fibrous capsule of the lymph node. Collagen 1 IHC stain, 5x objective magnification.

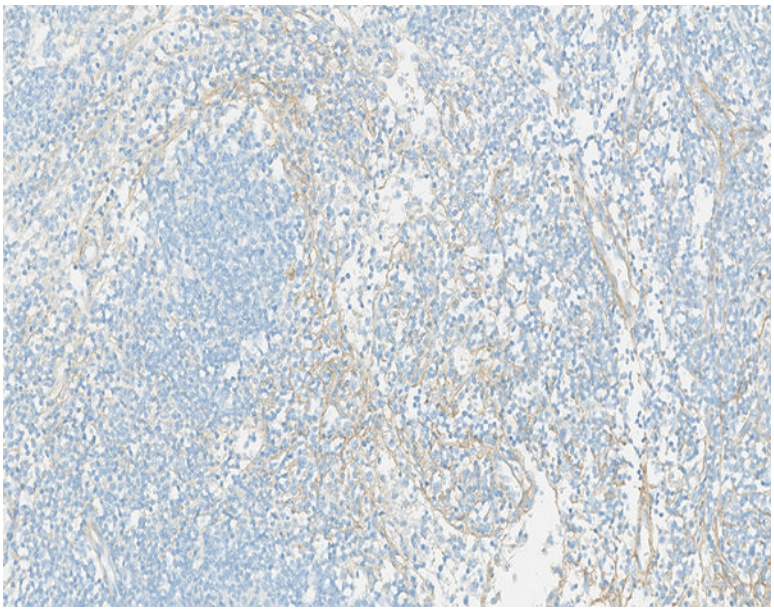

Figure 14d.
Higher magnification of the lymph node shown in the previous image has thin collagenous fibrils separating the cellular elements of the cortex. Collagen 1 IHC stain, 10x objective magnification.

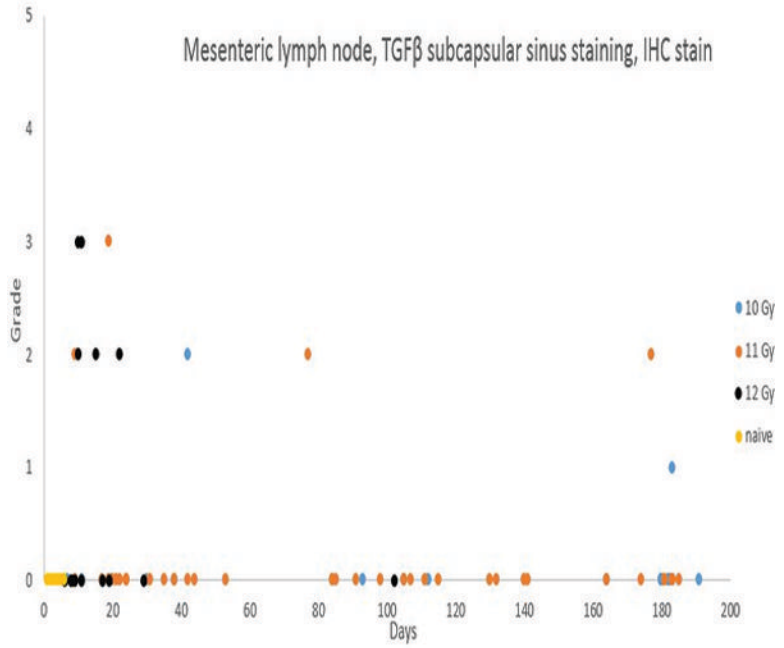

Figure 15a.

Cells expressing transforming growth factor-beta (TGFβ) in the subcapsular sinuses of mesenteric lymph nodes were observed most frequently in animals necropsied during the first 30 days post-irradiation. This cellular population was presumed to be derived from inflammatory cells that transited from the intestine to the mesenteric lymph nodes.

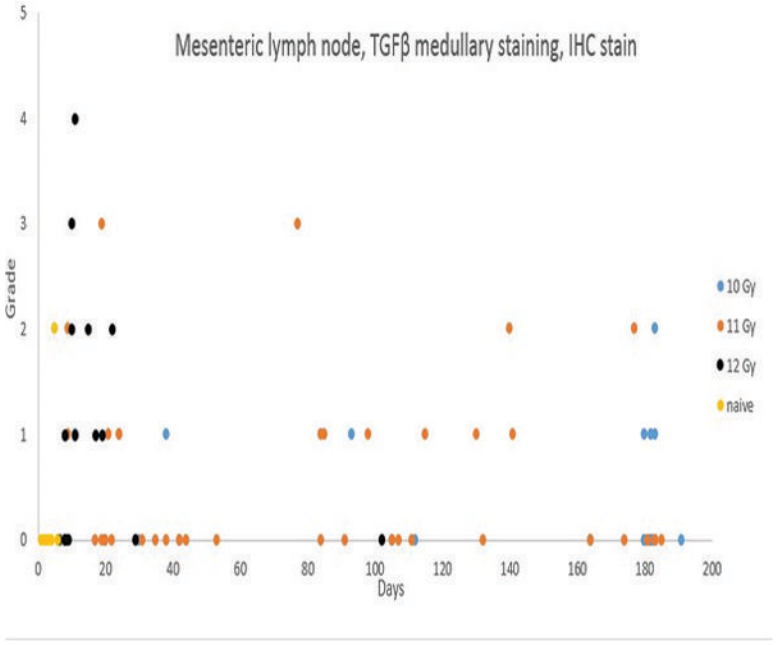

Figure 15b.

Cells expressing transforming growth factor-beta (TGFβ) in the medullary region of mesenteric lymph nodes were observed most frequently in animals necropsied during the first 30 days post-irradiation, but TGFβ expression continued in a subset of animals throughout the observation period. The greater expression of TGFβ in the lymph nodes parallels the severity of the radiation-associated intestinal lesions in animals irradiated at 12 Gy.

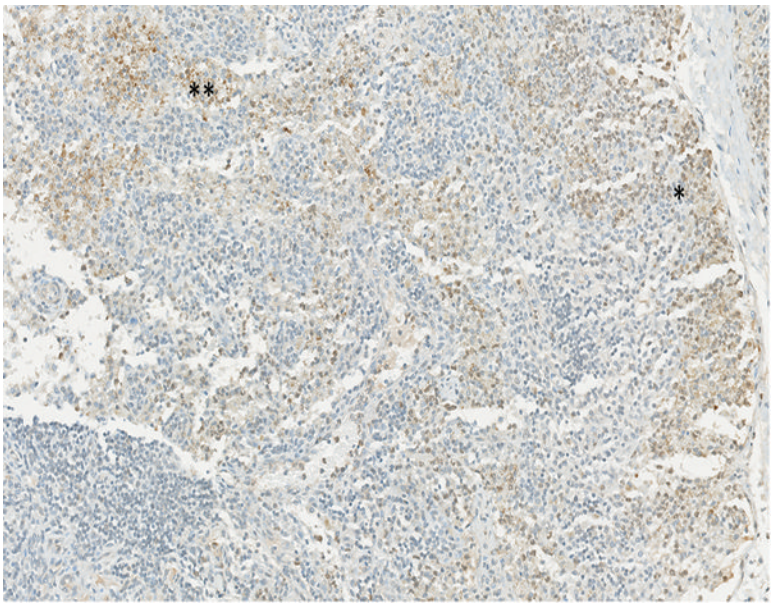

Figure 15c.

The mesenteric lymph node of a male rhesus macaque collected at day 11 following irradiation at 12 Gy has expression of transforming growth factor-beta (TGFβ) in cells located in both the subcapsular (*) and medullary (**) regions. TGFβ IHC stain, 15.1x objective magnification.

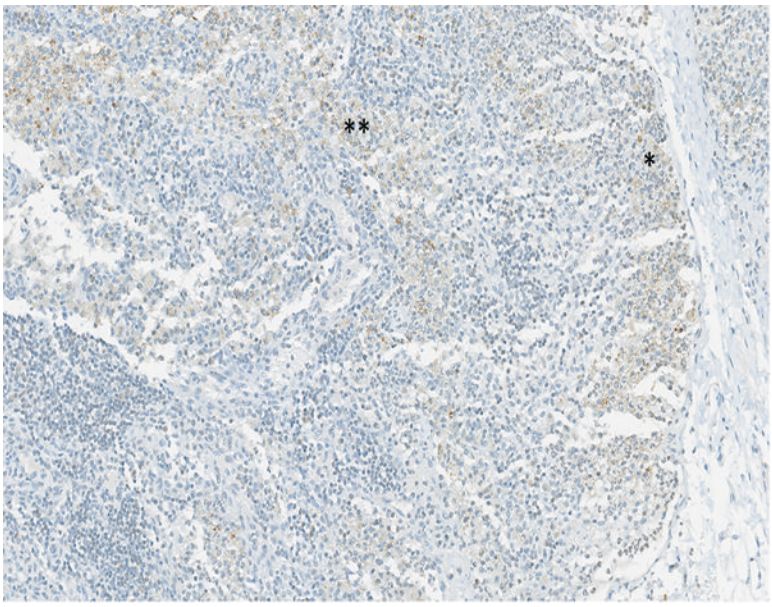

Figure 15d.

The mesenteric lymph node of the same male rhesus macaque presented in Figure 15c has moderate expression of connective tissue growth factor (CTGF) in both the subcapsular (*) and medullary (**) regions. The mesenteric lymph node of this animal also had grade 5 MxA expression, grade 2 LPS core expression, and grade 4 lymphoid depletion and grade 3 sinus histiocytosis on routine H&E staining. Immunohistochemical staining revealed no evidence of collagen deposition in the lymph node. CTGF IHC stain, 15x objective magnification.

Table 1

Histological and Immunohistochemical Stains on Colon, Jejunum and Mesenteric Lymph Node

Histochemical stains			
	Jejunum	Colon	Mesenteric Lymph Node
Hematoxylin & eosin	X	X	X
Masson's trichrome	X	X	X
Toluidine blue	X	X	X
PAS/Alcian blue	X	X	
Lendrum-Paneth cells	X		
Immunohistochemical stains			
α-SMA	X	X	X
Tryptase	X	X	X
Collagen 1	X	X	X
TGFb	X	X	X
CTGF	X	`X	X
Myeloperoxidase	X	X	X
MxA	X	X	X
LPS core	X	X	X
CD3	X	X	X
CD13	X	X	X
Ki67	X	X	
IL-22	X	X	
IL-22R	X	X	
Bmi-1	X	X	

Table 2

Necropsy Date Related to Radiation Dose

Radiation dose (Gy)	**10**	**11**	**12**
Number of animals	**30**	**42**	**17**
Necropsy dates[a]			
1–10	1	2	8
11–20	3	4	5
21–30	1	4	2
31–40	1	3	
41–50	1	2	
51–60		1	
61–70			
71–80		1	
81–90		3	1
91–100	1	4	
101–110	1	3	1
111–120	2		
121–130		1	
131–140	1	4	
141–150		1	
151–160			
161–170	1	3	
171–180	4		
181–191	13	6	

[a]=post-irradiation days when animals died or were euthanized